Corresponding author
Prof. Dr. H.V. Klapdor-Kleingrothaus
Max-Planck-Institut für Kernphysik
Saupfercheckweg 1
D-69117 HEIDELBERG
GERMANY
Phone Office: +49-(0)6221-516-262
Fax: +49-(0)6221-516-540
email: klapdor@gustav.mpi-hd.mpg.de

Data Acquisition and Analysis of the ^{76}Ge Double Beta Experiment in Gran Sasso 1990-2003

H.V. Klapdor-Kleingrothaus [1] A. Dietz, I.V. Krivosheina [2] and O. Chkvorets

Max-Planck-Institut für Kernphysik, PO 10 39 80, D-69029 Heidelberg, Germany

Abstract

Data acquisition in a long running underground experiment has its specific experimental challenges, concerning data acquisition, stability of the experiment and background reduction. These problems are addressed here for the HEIDELBERG-MOSCOW experiment, which collected data in the period August 1990 - May 2003. The measurement and the analysis of the data is presented. The duty cycle of the experiment was ∼80%, the collected statistics is 71.7 kg y. The background achieved in the energy region of the Q value for double beta decay is 0.11 events/ kg y keV. The two-neutrino accompanied half-life is determined on the basis of more than 100 000 events. The confidence level for the neutrinoless signal has been improved to a 4σ level.

[1] Spokesman of HEIDELBERG-MOSCOW (and GENIUS) Collaboration,
E-mail: klapdor@gustav.mpi-hd.mpg.de,
Home-page: *http : //www.mpi − hd.mpg.de.non_acc/*
[2] On leave of the Radiophysical-Research Institute, Nishnii-Novgorod, Russia

1 Introduction

Since 40 years huge experimental efforts have gone into the investigation of nuclear double beta decay which probably is the most sensitive way to look for (total) lepton number violation and probably the only way to decide the Dirac or Majorana nature of the neutrino. It has further perspectives to probe also other types of beyond standard model physics. This thorny way has been documented recently in some detail [33,69].

The half-lives to explore lying, with the order of 10^{25} years, in a range on 'half way' to that of proton decay, the two main experimental problems were to achieve a sufficient amount of double beta emitter material (source strength) and to reduce the background in such experiment to an extremely low level. In both directions large progress has been made over the decades. While the first experiment using source as detector [59], had only grams of material to its disposal (10.6 g of CaF_2), in the last years up to more than 10 kg of enriched emitter material have been used. Simultaneously the background of the experiments has been reduced strongly over the last 40 years. E.g. compared to the first Germanium $\beta\beta$ experiment [81], working still with natural Germanium, containing the double beta emitter ^{76}Ge only with 7.8%, 40 years later the background in the HEIDELBERG-MOSCOW experiment is reduced by a factor of 10^4.

Nevertheless experiments have to run over years to collect sufficient statistics and this led to other experimental challenges: stable data acquisition and calibration over long time periods (more than a decade in the HEIDELBERG-MOSCOW experiment). The final dream behind all these efforts was less to see a standard-model allowed second-order effect of the weak interaction in the nucleus - the two-neutrino-accompanied decay mode - which has been observed meanwhile for about 10 nuclei - to observe neutrinoless double beta decay, and with this a first hint of beyond standard model physics, yielding at the same time a solution of the absolute scale of the neutrino mass spectrum.

In this paper we describe how these challenges have been mastered in the HEIDELBERG-MOSCOW experiment, which is running in the Gran Sasso Underground Laboratory since August 1990, and which is now, together with the R. Davis ^{37}Cl solar neutrino experiment [61], the Baksan Neutrino Scintillation telescope [62] which saw together with Kamiokande and IMB the first Supernovae neutrinos [63,64], Kamiokande and SuperKamiokande [65], Gallex (GNO) [66] and SAGE [66], and DAMA [104], one of the long-running underground experiments.

In our last publications [3,1,2] we presented an analysis of the data taken until May 2000. Since then we have taken three more years of data. In this paper

we report the result of the measurements over the full period August 1990 until May 2003. The better quality of the new data and of the present analysis, which has been improved in various respects, allowed us to significantly improve the investigation of the neutrinoless double beta decay process, and to deduce more stringent values of its parameters.

2 Performance of the Experiment and Data Taking

2.1 General

The HEIDELBERG-MOSCOW experiment, proposed already in 1987 [5] is looking, with enriched Germanium detectors, for double beta decay of ^{76}Ge since August 1990 in the Gran Sasso Underground Laboratory. It is using the largest source strength of all double beta experiments at present, and has reached a record low level of background, not only for Germanium double beta decay search. It has demonstrated this during more than a decade of measurements and is since 10 years the most sensitive double beta decay experiment worldwide. The experiment is since 2001 operated only by the Heidelberg group, which also performed the analysis of the experiment from its very beginning. The experiment presents - as a long-running low-level underground experiment - specific extreme challenges concerning e.g. stability of the data acquition and the background reduction.

In this paper we give a description of the experimental procedure, concentrating on the specific features and challenges of the data acquisition and background reduction, present the data taken until May 20, 6:57, 2003 - with a total statistics of 56.66 kg y for the period November 1995 - May 2003 and of 71.71 kg y for the period August 1990 - 2003 (about 17 kg y more than analysed in 2001 [1–3]), and we present their analysis.

The experiment is carried out with five high-purity p-type detectors of Ge enriched to 86% in the isotope ^{76}Ge (in total 10.96 kg of active volume). These were the first enriched high-purity Ge detectors ever produced. It should be stressed that by the procedure of zone-refinement, used for production of the high-purity Germanium single-crystals, such detector material probably is the cleanest material of any kind, which has ever been produced in commercial volume (impurity level as low as $\sim 10^9$ atoms/cm^2). Since impurities tend to be more soluble in the molten germanium than in the solid, impurities are transfered to the molten zone and are swept from the sample (see e.g. [45]). So, the experiment starts from the cleanest thinkable source of double beta emitter material, which at the same time is used as detector of $\beta\beta$ events.

Some description of the experimental details has been given already in [6–8]. Here we give some new information on the most important points.

1. Since the sensitivity for the $0\nu\beta\beta$ half-life is

$$T_{1/2}^{0\nu} \sim a \times \epsilon \sqrt{\frac{Mt}{\Delta E B}} \tag{1}$$

(and $\frac{1}{\sqrt{T^{0\nu}}} \sim \langle m_\nu \rangle$), with a denoting the degree of enrichment, ϵ the efficiency of the detector for detection of a double beta event, M the detector (source) mass, ΔE the energy resolution, B the background and t the measuring time, the sensitivity of our 11 kg *of enriched* ^{76}Ge experiment corresponds to that of an at least 1.2 ton *natural* Ge experiment. After enrichment - the other most important parameters of a $\beta\beta$ experiment are: energy resolution, background and source strength.

2. The high energy resolution of the Ge detectors of 0.2% or better, assures that there is no background for a $0\nu\beta\beta$ line from the two-neutrino double beta decay in this experiment, in contrast to most other present experimental approaches, where limited energy resolution is a severe drawback.

3. The efficiency of Ge detectors for detection of $0\nu\beta\beta$ decay events is close to 100 % (95%, see [29](a)).

4. The source strength in this experiment of 11 kg is the largest source strength ever operated in a double beta decay experiment.

5. The background reached in this experiment, is 0.113 ± 0.007 events/kg y keV (in the period 1995-2003) in the $0\nu\beta\beta$ decay region (around $Q_{\beta\beta}$). This is the lowest limit ever obtained in such type of experiment.

6. The statistics collected in this experiment during 13 years of stable running is the largest ever collected in a double beta decay experiment. The experiment took data during $\sim$ 80% of its installation time.

7. The Q value for neutrinoless double beta decay has been determined recently with high precision [41–44].

2.2 Experimental Details

Active Mass, Enrichment, Shielding. All detectors (whose technical parameters are given in Table 1, see [6]), are enriched in ^{76}Ge to 86-88% (natural abundance 7.8%). The degree of enrichment has been checked by investigation of tiny pieces of Ge *after* crystal production using the Heidelberg MP-Tandem

accelerator as a mass spectrometer. The detectors, except detector No. 4, are operated in a common Pb shielding of 30 cm, which consists of an inner shielding of 10 cm radiopure LC2-grade Pb followed by 20 cm of Boliden Pb. The whole setup is placed in an air-tight steel box and flushed with radiopure nitrogen in order to suppress the ^{222}Rn contamination of the air. The shielding has been improved in the course of the measurement. The steel box is since 1994 centered inside a 10-cm boron-loaded polyethylene shielding to decrease the neutron flux from outside. An active anticoincidence shielding is placed on the top of the setup since 1995 to reduce the effect of muons. Detector No. 4 is installed in a separate setup, which has an inner shielding of 27.5 cm electrolytical Cu, 20 cm lead, and boron-loaded polyethylene shielding below the steel box, but no muon shielding. Fig. 1 gives a view of the experimental setup.

Fig. 1. The HEIDELBERG-MOSCOW $\beta\beta$-experiment in the Gran Sasso (top), and four of the enriched detectors during installation (bottom left). The fifth detector is installed in an extra shielding using electrolytic copper as inner shield (bottom right).

The setup has been kept hermetically closed since installation of detector 5 in February 1995. Since then no radioactive contaminations of the inner of the experimental setup by air and dust from the tunnel could occur. Before this time the shielding of the experiment was opened several times to add new detectors.

Table 1
Technical parameters of the five enriched ^{76}Ge detectors.

	Total	Active	Enrichment	
Detector Number	Mass [kg]	Mass [kg]	in ^{76}Ge [%]	PSA
No. 1	0.980	0.920	85.9 ± 1.3	no
No. 2	2.906	2.758	86.6 ± 2.5	yes
No. 3	2.446	2.324	88.3 ± 2.6	yes
No. 4	2.400	2.295	86.3 ± 1.3	yes
No. 5	2.781	2.666	85.6 ± 1.3	yes

Control of stability of the experiment and data taking. To control the stability of the experiment, a calibration with a ^{228}Th and a ^{152}Eu+^{228}Th, has been done weekly. High voltage of the detectors, temperature in the detector cave and the computer room, the nitrogen flow flushing the detector boxes to remove radon, the muon anticoincidence signal, leakage current of the detectors, overall and individual trigger rates are monitored daily. The energy spectrum is taken in parallel in 8192 channels in the range from threshold up to about 3 MeV, and in a spectrum up to about 8 MeV.

Data collection since November 1995 is done by a CAMAC system, and CETIA processor in event by event mode. To read out the used 250 MHz flash ADCs of type Analog Devices 9038 JE (in DL515 modules), which allow digital measurement of pulse shapes for the four largest detectors, a data acquisition system on VME basis has been developed [29](c). The resolution of the FADC's is 8 bit, and thus not sufficient for a measurement of energies. The energy signals for high and low-energy spectra are recorded with 13 bit ADC's developed at MPI Heidelberg. The preamplifier signal, which is proportional to the collected charge, is differentiated by Timing Filter Amplifieres (TFA's). Every 4 nsec the voltage read at the TFA's is recorded. In the event by event mode also the other parameters of each event such as time, voltage at the detectors, temperature at three measuring points, information from muon shield and other parameters of the electronic crates are recorded, such as ADC values. For this purpose a monitor card developed at MPI containing four 12 bit digital-analog converters, four TTL signal exits and a fast digital-analogue converter (10 nsec rise time) is used. The recorded time development of each event (pulse shape) is then analysed later off-line. Fig. 2 shows (in a simplified way) the trigger logics for LIST and Single-Mode operation for one detector (from [29](c)). For details we refer to [29](c). To have an additional quantitive check for the quality of each pulse, the 'Energy over Integral' (EoI) value is calculated by dividing the deposited energy in the ADC by the area of the pulse in the timing channels. The acquisition system used *until* 1995 (VAX/VMS) did not allow to measure the pulse shapes of all detectors because of the too low data transfer rates.

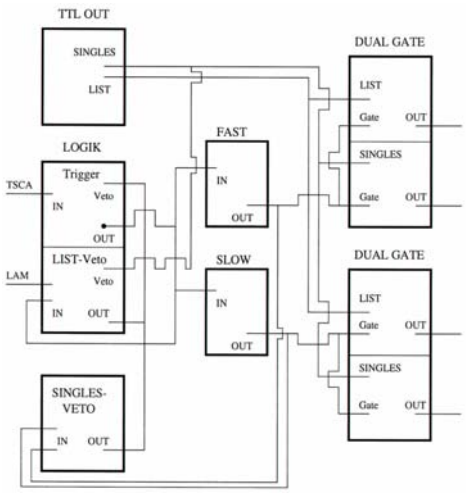

Fig. 2. The trigger logics for LIST and Single-Mode operation for one detector (from [29](c)).

After conversion of the original binary files, the data for each event are stored in ASCII format: the number of the event, the identification number of the detector in which the event occurred, the time of the event, the time since the last muon veto signal (if less than $20\mu s$, otherwise zero), the Energy over Integral value, the results of the network obtained from the single SSE library, the result of the network obtained with mixed SSE library [28], the rise time of the event and finally the *broad* value of the analysis method of [26,27].

In total we have taken 2142 runs (10 513 data sets for the five detectors) since 1995 (*without* calibration measurements), the average length of which was about one day.

From these raw data runs and data sets only those are considered for further analysis which fulfill the following conditions:

(1) no coincidence with another Ge detector;
(2) no coincidence with plastic scintillator (muon shield) (see Fig. 3);
(3) no deviation from average count rate of each detector more than $\pm 5\sigma$ (see Fig. 4);
(4) only pulses with ratios of the energy determined in the spectroscopy branch, and the area under the pulse detected in the *timing* branch (EoI values [28]), within a $\pm 3\sigma$ range around the mean value for each detector are accepted (see Fig. 5);
(5) we ignore for each detector the first 200 days of operation, corresponding to about three half-lifes of ^{56}Co ($T^{0\nu}_{1/2}$=77.27 days), to allow for some decay of short-lived radioactive impurities;
(6) ADC's or other electronics units were working properly (corrupted data are excluded).

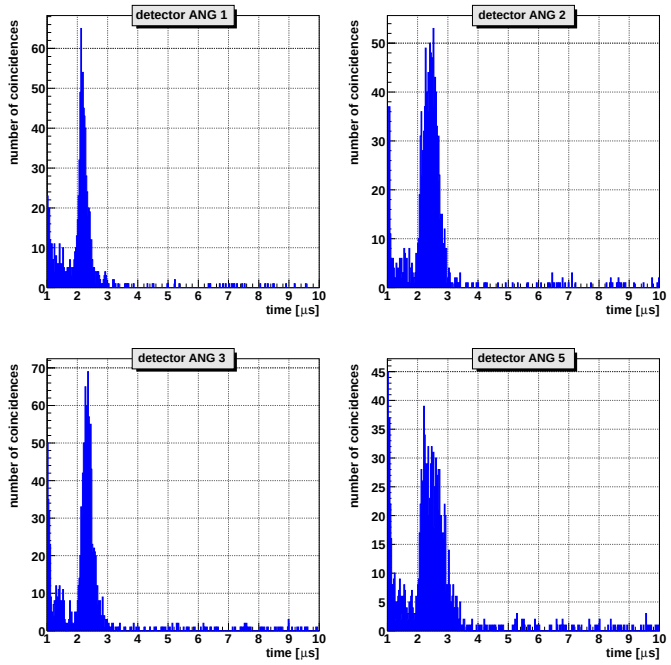

Fig. 3. Abundance of coincidences between muon-detector and Ge detectors, in the period 1995-2003. Shown is the time difference between signals from a detector and from muon shield (the latter electronically delayed). The peak at $\sim$2.2μsec corresponds to muon-shield-Ge-detector coincidences. Excluded from analysis as muon-induced events are signals within the range 1-5 μsec.

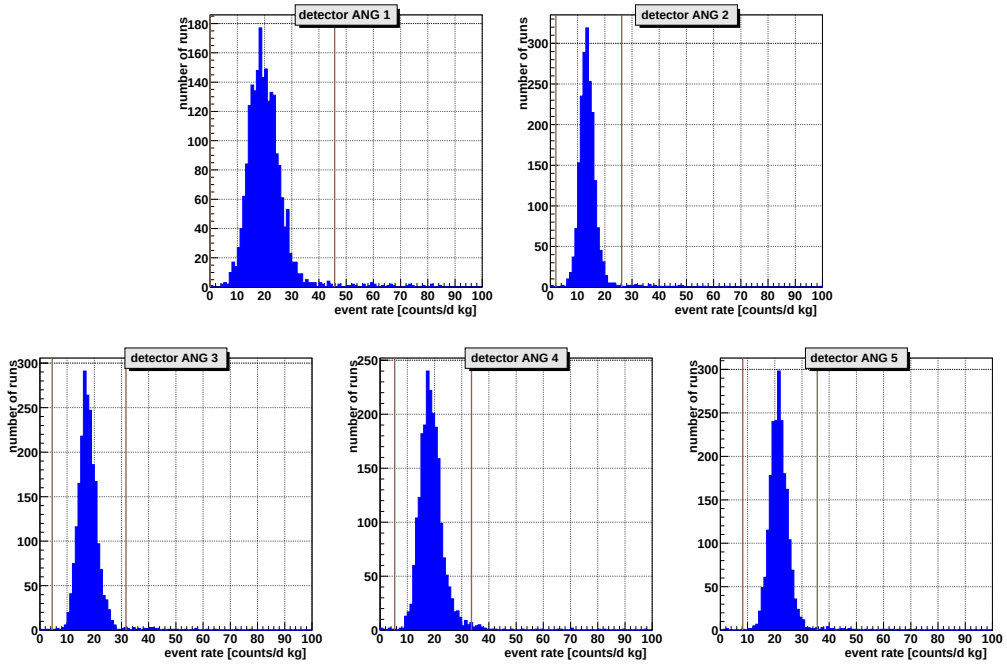

Fig. 4. Shown is the distribution of the rates (in counts/d kg) for each detector over the energy range 400 - 2700 keV, and the range of $\pm 5\sigma$ deviation (brown vertical lines) from the average value for the period 1995-2003.

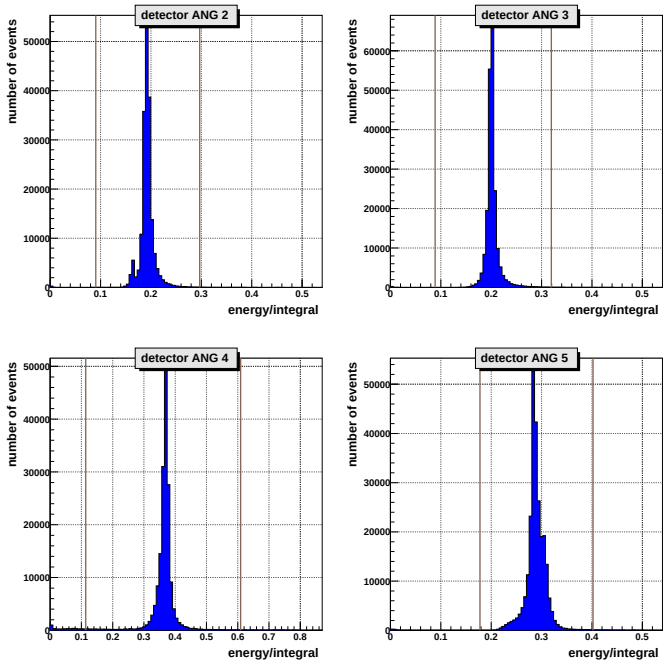

Fig. 5. Distribution of EoI values for the individual detectors and the $\pm 3\sigma$ accepted range (between brown vertical lines), for the period 1995-2003.

Table 2 gives an overview of the classification of the raw data.

After rejection of corrupted runs (792 runs, $\sim$9.7% of the data, see Table 2) there remain 858 491 events. After rejection of events being coincident with other Ge detectors and with muon shield (in total 25 470 events) we have 833 021 events. Excluding runs with a deviation of the average rate of each detector, by more than $\pm 5\sigma$, we have 800 099 events, and rejecting events with not proper EoI value leaves finally 786 652 events. From these we find in the range 2000 to 2060 keV around $Q_{\beta\beta}$ – 562 events.

Table 2
The data acquisition of the HEIDELBERG-MOSCOW experiment during 1995 - 2003. *) events show up partly in μ *and* Ge-Ge coincidence, therefore *in total* 25 470 events.

	Data Sets	Events
Full measurement	10 513	951 044
Corrupted data sets	792	92 553
Rate $> \pm 5\sigma$	151	32 922
Muon coincidence *		3 672
Ge - Ge coincidence *		23 563
EoI selection		13 158
Data used	9 570	786 941

Q **Value.** The expectation for a $0\nu\beta\beta$ signal would be a sharp line at the Q value of the process. Earlier measurements gave $Q_{\beta\beta} = 2040.71 \pm 0.54$ [44], 2038.56 ± 0.32 [42], and 2038.668 ± 2.142 [43]. The recent precision measurement of [41] gave a value of 2039.006 ± 0.050 keV.

Time structure of the events. In addition to the total spectrum, the time structure of the pulses have been measured for later off-line pulse shape analysis. As mentioned above, for this purpose the output of the charge-sensitive preamplifiers was differentiated with 10-20 ns sampled with 250 MHz. Fig. 6

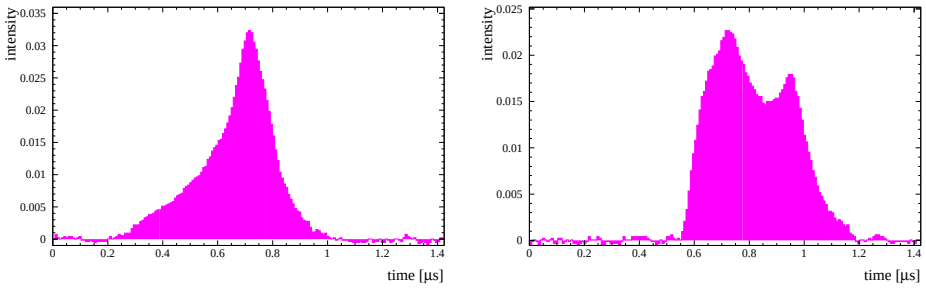

Fig. 6. Left: Shape of an event classified as SSE by all three methods of pulse shape discrimination. Right: Shape of an event classified as multiple site event (MSE) by all three methods.

shows typical examples of measured time structures. The $0\nu\beta\beta$ signal should be in simplified view a line consisting mainly of single site events (SSE) [26],[29](a,c,d) confined to a few mm region in the detector corresponding to the track length of the emitted electrons. In this ideal case, a line of single site events should sit on some background of multiple site events (MSE) but also single site events in the spectrum, the latter coming to a large extent from the Compton continuum of the 2614 keV γ-line from ^{208}Tl (most of the Compton continuum consists [29,46] of single Compton scatterings followed by escape of the scattered γ-ray (single site events) (see Fig. 7)). However, this idealized picture is not fully realized in nature. That we cannot expect a class of 100% pure SSE events for the $0\nu\beta\beta$ signal is obvious from simulations. From simulation we expect that part of the double beta single site events should be seen as MSE. Simulations show that the maximum interaction distance of electrons may exceed appreciably the maximum range of electrons in Germanium [29,84]. A long tail of this distribution is connected with bremsstrahlung gamma quanta. According to simulations [29](a) this amounts to 5.1% of the $0\nu\beta\beta$ events, and in total 13.1% of the $0\nu\beta\beta$ events should be recognized as MSE events. On the other hand also real multiple site events produced by γ-quanta could be observed as SSE if energy deposition takes place at the same equipotential surface, at locations in the detector far away from another. The situation is further complicated by the fact, that the pulse shapes of a given class of events will in addition show some dependence on the location in the crystal.

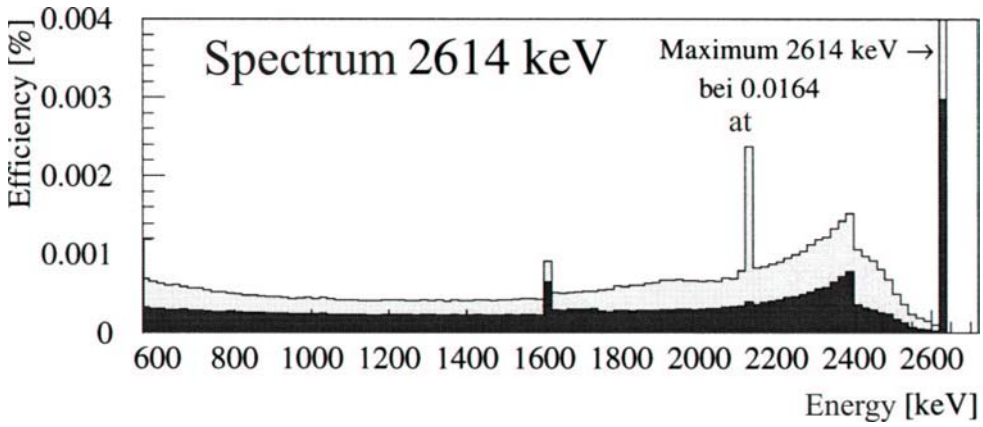

Fig. 7. Simulated spectrum for the γ-line at 2614 keV from a ^{228}Th source in a Germanium detector. The light shaded area denotes the full spectrum consisting of multiple and single site events, the dark area only the single site events. The full energy peak at 2614 keV consists mainly of MSE (about 80% MSE and 20% SSE), the single escape peak at 2103 keV of almost 100% MSE, while the 1592 keV double escape peak is practically fully single site (from [29](a), see also [40,46]).

We have tried different methods to get some selection of single site events in the following way. The first one relies on the socalled 'broadness' of the charge pulse maximum [26,27]. The second and third one are based on neuronal networks [28] and differ by using one or two lines for neuronal training (single or mixed SSE library, respectively). All three methods we tried to 'calibrate' with the known double escape (mainly SSE) line at 1592.5 keV and the total absorption (mainly MSE) γ-line at 2614.5 keV of a ^{228}Th source (see Fig. 7 and Fig. 30), and partly with the double escape line of the 3253.4 keV line of ^{56}Co at 2231.4 keV (see [26–28]). For our purpose, this tacidly assumes, that the signal produced by a γ-quant absorbed by electron pair creation behaves identical to a double beta decay signal. This is of course not fully the case. In this sense at present, all of these methods, and combinations of them, are, for application to double beta decay, still in a pioneering stage (see section 4). Work on improvement particularly of the neuronal net methods is, therefore, in progress.

Background from two-neutrino double beta decay. Because of the high resolution of the Ge detectors *no* background, (precisely $5.5\times\ 10^{-9}$ events in the area 2035 - 2039.1 keV), in the range of a potential $0\nu\beta\beta$ line at $Q_{\beta\beta}$ is expected from the two-neutrino double beta decay, for which the half-life has been determined from the same experiment to be $(1.74^{+0.18}_{-0.16}) \times 10^{21}$ y [15,6]. For a resolution of a few hundred keV, as realized in some experiments, the contribution of $2\nu\beta\beta$ events in the same range would be untolerable (150 events in the range 1800 - 2039 keV).

Other background. Because of the big peak-to-Compton ratio of the large

detectors, external γ activities are relatively easily identified, since their Compton continuum is to a large extent shifted into the peaks. The background identified by the measured γ lines in the spectrum consists of:

(1) primordial activities of the natural decay chains from ^{238}U, ^{232}Th, and ^{40}K;
(2) anthropogenic radio nuclides, like ^{137}Cs, ^{134}Cs, ^{125}Sb, ^{207}Bi;
(3) cosmogenic isotopes, produced by activation due to cosmic rays.

The activity of these sources in the setup is measured directly and can be located due to the measured and simulated relative peak intensities of these nuclei.

Hidden in the continuous background are the contributions of:

(4) the bremsstrahlungs spectrum of ^{210}Bi (daughter of ^{210}Pb);
(5) the overwhelming part of elastic and inelastic neutron scattering, and
(6) direct muon-induced events.

External α and β activities are shielded by the 0.7-mm inactive zone of the p-type Ge detectors on the outer layer of the crystal. The enormous radiopurity of HP-germanium is proven by the fact that the detectors No. 1, No. 2 and No. 3 show no indication of any α peaks in the measured data. Therefore no contribution of the natural decay chains can be located inside the crystals. Detectors No. 4 and No. 5 seem to be slightly contaminated with ^{210}Pb on the level of few μBq/kg, most likely surface contaminations at the inner contact. This contamination was identified by a measured α peak in the background spectrum at 5.305 MeV of the daughter ^{210}Po and the constant time development of the peak counting rate. There is no contribution to the background in the evaluation areas of interest of the experiment due to this activity.

For a detailed description of the background of the experiment and its extensive simulation with GEANT4 we refer to [15]. We mention here only that *all* visible background lines in the sum spectrum up to 2020 keV (see Figs. 15,16) are identified, and that subtraction of the background simulated on this basis allows to deduce the half-life for two-neutrino decay to be [15] $T^{2\nu}_{1/2} = (1.74^{+0.18}_{-0.16}) \times 10^{21}\ years$. This half-life determination is based on $\sim$ 114 000 events [15], which may be compared to the about 35 events from which the first $2\nu\beta\beta$ spectrum had to be composed 15 years ago [80].

We show here only, because of its relevance in the later discussion (see section 4), the simulated background in the range around $Q_{\beta\beta}$ (see Fig. 8). The different background components are shown in different colours [15].

The most significant background contribution between 2000 and 2100 keV comes from the decay of the isotope ^{208}Tl. This isotope is part of the natural ^{232}Th decay chain and has a strong γ–peak at 2614 keV. The background contribution observed between 2000 and 2100 keV is part of the Compton continuum of that peak and therefore flat (see also Fig. 7). The contributions

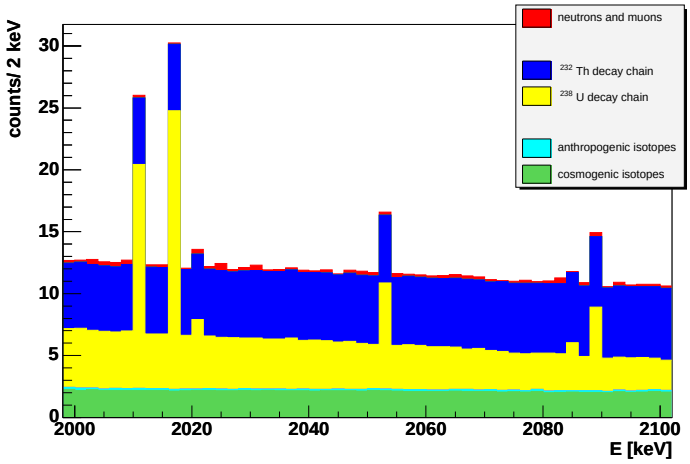

Fig. 8. Simulated background components in the energy region from 2000 to 2100 keV around the Q-value for double beta decay at 2039 keV for all five detectors in the period 20.11.1995 to 16.04. 2002 (49.59 kg y)). A bin width of 2 keV was chosen (from Ref. [15]). The simulated spectrum *is not* folded with the energy resolution of the detectors.

of the ^{238}U natural decay chain are coming mainly from ^{214}Bi, the cosmogenic contribution arises from mainly ^{60}Co produced by spallation during production of the crystals (for details about the contribution of spallation products to the background in Ge detectors see [107]).

The γ–peaks observed in the simulated spectrum near $Q_{\beta\beta}$ are emitted from the isotope ^{214}Bi. So from ^{214}Bi (^{238}U-decay chain) in the vicinity of the Q-value of the double beta decay of $Q_{\beta\beta} = 2039$ keV, according to the Table of Isotopes [39], weak lines should be expected at 2010.7, 2016.7, 2021.8 and 2052.9 keV. Additional weak lines at 2034.744 and 2042 keV from the short-lived cosmogenic nuclide ^{56}Co, which were still visible in the sum spectrum of [29](c), are not visible any more in the actual sum spectrum.

As seen from Fig. 8, there are no background γ-lines to be expected at the position of an expected $0\nu\beta\beta$ line, according to our Monte Carlo analysis of radioactive impurities in the experimental setup [29,15] and according to the compilations in [39].

It should be especially noted, that also neutron capture reactions $^{74}Ge(n,\gamma)^{75}Ge$ and $^{76}Ge(n,\gamma)^{77}Ge$ and subsequent radioactive decay have been simulated by GEANT4 in [15]. The simulation yields, in the range of the spectrum 1990 - 2110 keV, for the total contribution from decay of ^{77}Ge 0.15 counts. So in particular, the 2037.8 keV transition in the γ-decay following β^- decay of ^{77}Ge [39] is not expected to be seen in the measured spectra.

Development of the experiment. Table 3 shows the collected statistics of

the experimental setup and of the background number in the different data acquisition periods for the five enriched detectors of the experiment for the total measuring time August 1990 to May 2003.

Table 3
Collected statistics and background numbers in the different data acquisition periods for the enriched detectors of the HEIDELBERG-MOSCOW experiment for the period 1990 - 2003. The life times of the experiment given in the second column *include* the data sets rejected according to Table 2.
*) Background determined by averaging counting rate in interval 2000-2100 keV (without PSA method).
**) From 11.1995 till 05.2003, background determined at $Q_{\beta\beta}$ from *fit* of spectrum in range 2000-2060 keV (with PSA method).

Detector Number	Life Time of all data		Life Time accepted for analysis		Date Start End	Background*) (counts/ keV y kg) 2000 - 2100 keV	PSA
	days	kg d	days	kg d			
1	1237.0	1138.04	930.9	856.43	8/90 - 8/95	0.31	no
2	1070.0	2951.06	997.2	2750.28	9/91 - 8/95	0.21	no
3	834.7	1939.84	753.1	1750.20	9/92 - 8/95	0.20	no
4	147.6	338.74	61.0	139.99	1/95 - 8/95	0.43	no
5	48.0	127.97	-	-	12/94 - 8/95	0.23	no
After summing of all 5 detectors over period 1990 - 1995, Accepted life time = **15.05 kg y**							
Full Setup, over period 1995 - 2003 **Four detectors in common shielding, one detector separate**							
1	2123.90	1967.25	2090.61	1923.36	11/95 - 5/03	0.20	no
2	1953.65	5427.94	1894.11	5223.96	11/95 - 5/03	0.11	yes
3	2120.22	4960.83	2079.46	4832.67	11/95 - 5/03	0.17	yes
4	2123.90	4907.44	1384.69	3177.86	11/95 - 5/03	0.21	yes
5	2110.66	5665.46	2076.34	5535.52	11/95 - 5/03	0.17	yes
After summing of all 5 detectors over period 1995 - 2003, Accepted life time = **56.655 kg y**, Background=**0.113 ±0.007 events/ keV y kg****, or 0.16 events/ keV y kg according to*							

Reliability of data equisition and data. We have carefully checked all data before starting the analysis. This is particularly important in such a long-running low-background experiment. Because of the general relevance of the present data, we show the situation for each detector. Fig. 9 shows the intensities of all 366 energy calibration runs as function of Runs

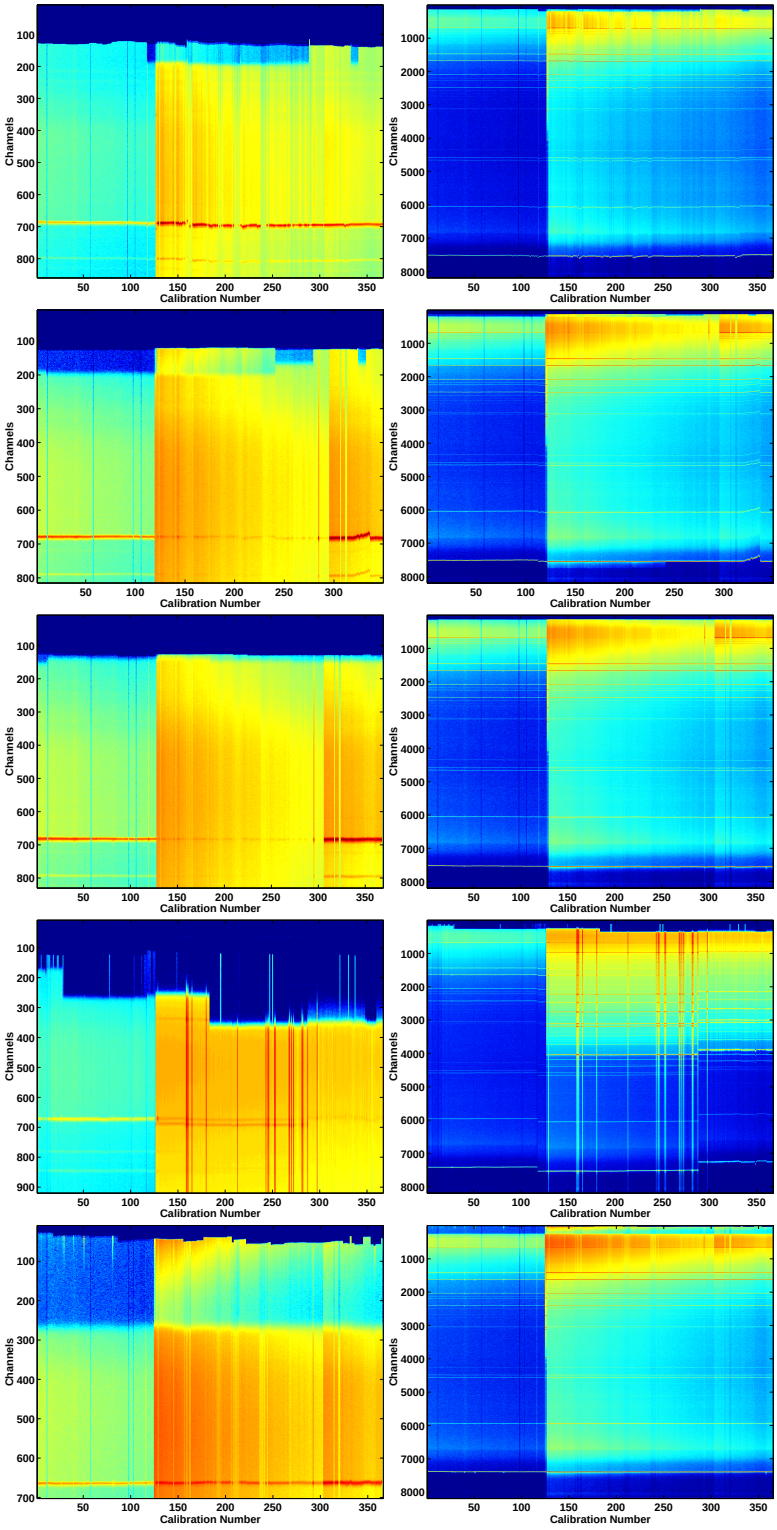

Fig. 9. The intensities of all $\sim$ 360 energy calibration runs for detectors 1,2,3,4,5 (from top to bottom) as function of Runs and channels. Colours indicate different intensities. Intensity increases from dark blue (zero events) to red. Horizontal lines correspond to lines in the Th source spectrum. No calibration of the energies of the individual calibration runs are made here.

and channels. Colours indicate different intensities. Horizontal lines correspond to γ-lines in the Th source spectrum. We see their position in general to be very stable even without any calibration of the individual runs. It is clearly visible that from calibration Run Nr. 1153 (29 April 1998), we used a *stronger* Th source. We see the proper operation of the thresholds in all ADC's (blue range - no events). Fig. 10 gives the number of events in a channel number of the low-energy branch ADC's against run number plane for all detectors, for the *data* used in the analysis. The behaviour of the thresholds corresponds to what is seen in Fig. 11, which shows the threshold ranges for detectors 4 and 5, from the list mode data acquisition of the measurement.

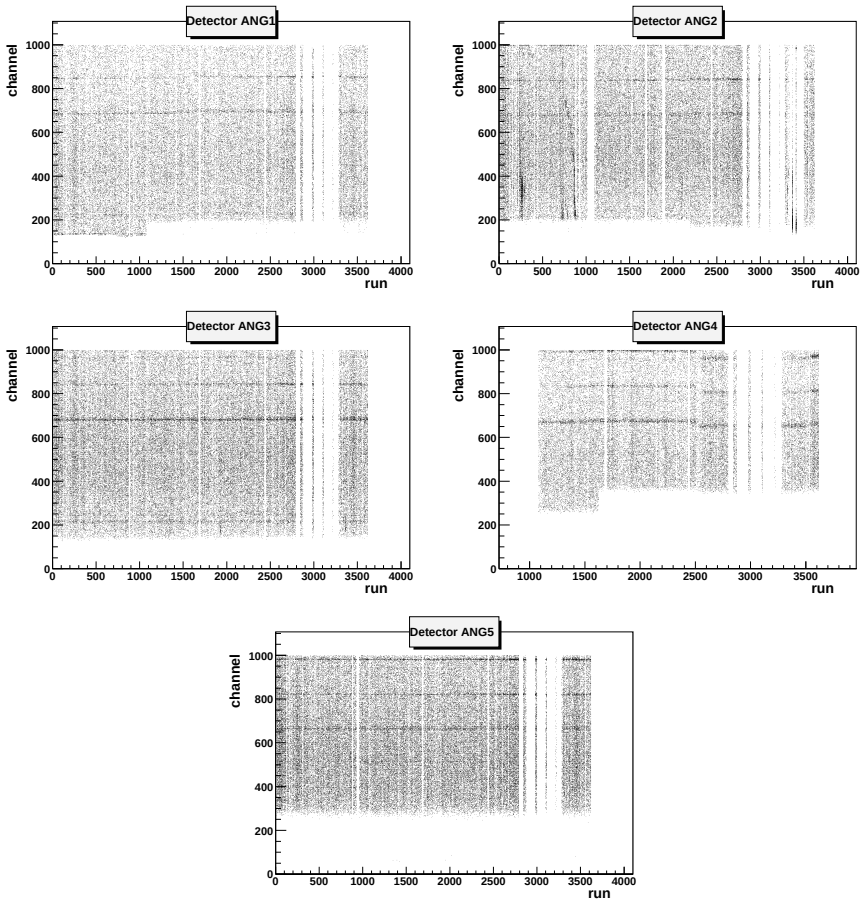

Fig. 10. The number of events in a channel number against Run number plane for all detectors, for the data used in the analysis (for period 1995 - 2003). The data are presented here *before* energy calibration, compare Figs. 26,27.

We also checked the arrival time distribution of the events, and proved that this is not affected by any technical operation during the measurement, such as the calibration procedure (introducing the Th source into the detector chamber through a thin tube) and simultaneously refilling of liquid nitrogen to the detectors etc. As example Fig. 12 (left) shows the arrival time distribution of all events observed in the energy interval $(2035.5 \div 2042.5)$ keV as function of

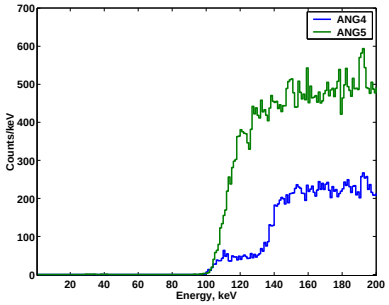

Fig. 11. Threshold ranges for detectors 4 and 5 in the spectrum measured during 1995 - 2003.

time after each calibration and refilling of liquid nitrogen (shown are the first 7 days after calibration and refilling. Note, that after calibration and refilling a new measurement is started after a waiting time of a few hours). No hint is seen for introduction of any radioactive material from the exterior is seen. The measured distribution corresponds to a uniform distribution in time on a 99% c.l. This has been proven by a Kolmogorov-Smirnov goodness-of-fit test of the hypothesis, that the measured cumulative distribution Fig. 12 (right) corresponding to the measured distribution of the events (see Fig. 12 left) corresponds to a random distribution in time.

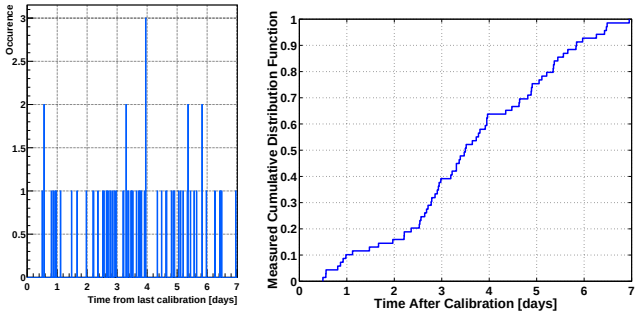

Fig. 12. Left: arrival time for all events in the interval 2035.5 - 2042.5 keV as function of time after the calibrations for the period 1995 - 2003 and the corresponding cumulative distribution (right) analyzed by the Kolmogorov-Smirnov test (see text).

Fig. 13 shows the range from 500 keV to 600 keV for the individual detectors measured in the period 1995 - 2003. The effect discussed in [84] (their Fig. 4) is not present in our analysis. Also the other effects discussed in [84] are not present in the analysis (see Figs. 9,10, 11, 13). A detailed analysis shows that these effects arise from including corrupt data into the analysis.

Fig. 14 shows that the high- and low-energy spectra taken simultaneously, overlap perfectly up to the end of the lower-energy spectrum at $\sim$3 MeV, proving consistency of the data collected in the low- and high-energy spectroscopy branch for all detectors.

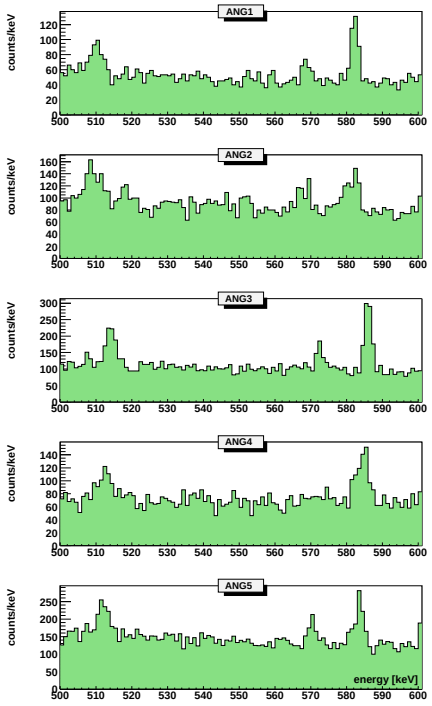

Fig. 13. Spectra for all five detectors obtained in the period 1995 - 2003 in the HEIDELBERG-MOSCOW experiment in energy intervall 500 - 600 keV.

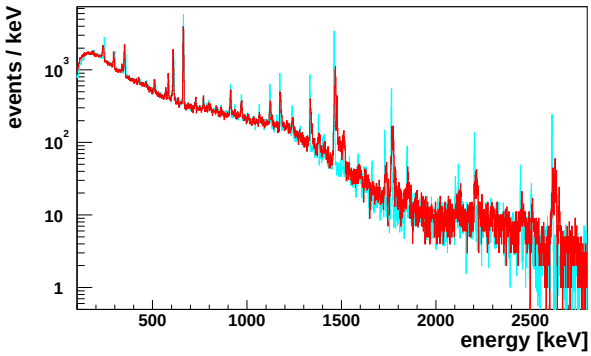

Fig. 14. Low- and High-energy measurements of the full spectrum, measured in the period November 1995 - May 2003.

3 Data and Analysis

Figs. 15, 16 show the total sum spectrum measured over the full energy range of all five detectors for the period August 1990 to May 2003. All identified lines are indicated with their source of origin (for details see [15],[29](e,f)).

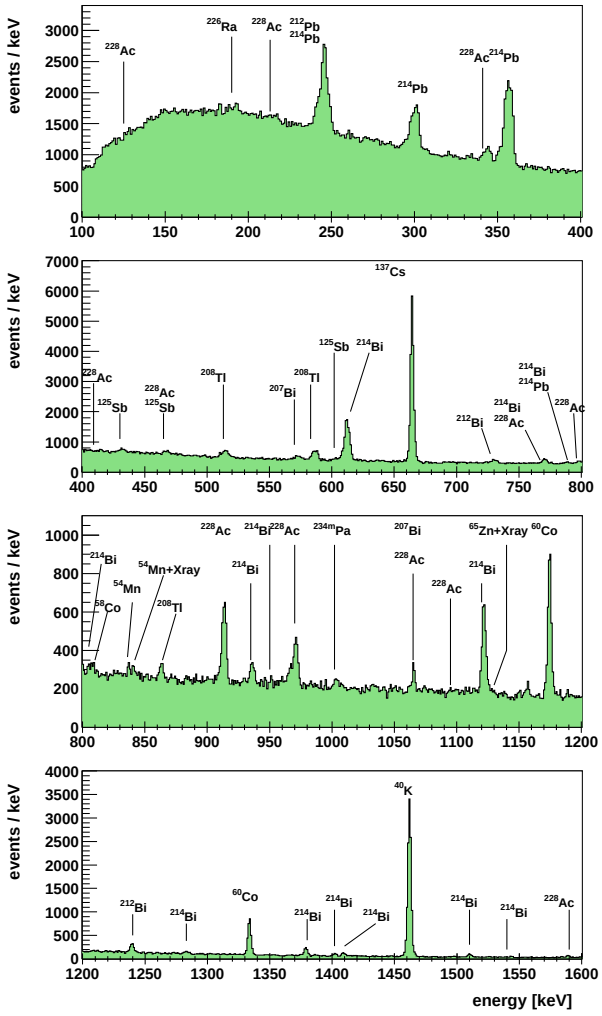

Fig. 15. The total sum spectrum measured over the full energy range (low-energy part) of all five detectors (in total 10.96 kg enriched in ^{76}Ge to 86%) - for the period August 1990 to May 2003.

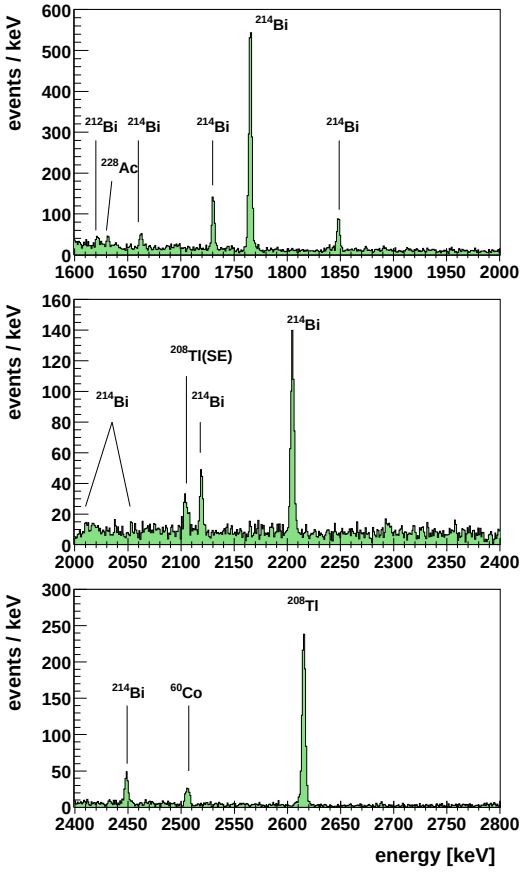

Fig. 16. The total sum spectrum measured over the full energy range (higher energy part) of all five detectors (in total 10.96 kg enriched in ^{76}Ge to 86%) - for the period August 1990 to May 2003.

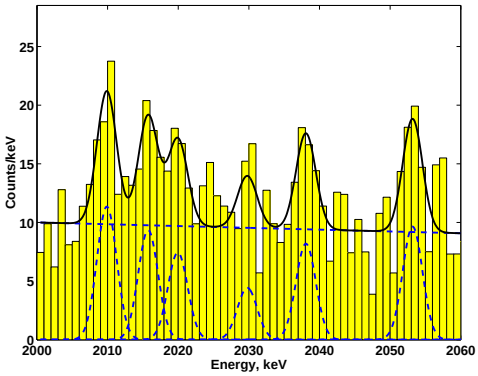

Fig. 17. The total sum spectrum of all five detectors (in total 10.96 kg enriched in ^{76}Ge), for the period November 1990 to May 2003 (71.7 kg y) in the range 2000 - 2060 keV and its fit (see section 3.2).

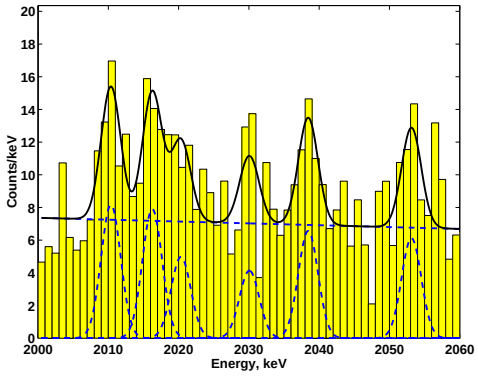

Fig. 18. The total sum spectrum of all five detectors (in total 10.96 kg enriched in ^{76}Ge), for the period November 1995 to May 2003 (56.66 kg y) in the range 2000 - 2060 keV and its fit (see section 3.2).

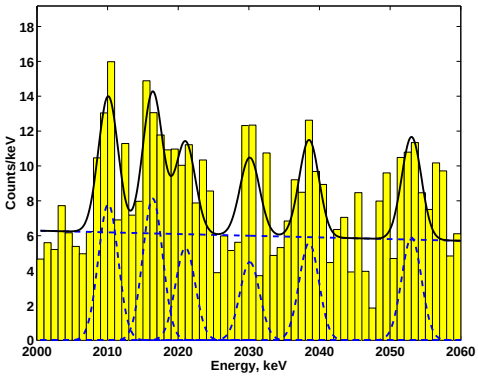

Fig. 19. Total spectrum in the range 2000 - 2060 keV obtained with detectors 2,3,4,5 (51.39 kg y) in the period November 1995 to May 2003, and its fit (see section 3.2).

Figs. 17,18 show the part of the spectrum around $Q_{\beta\beta}$, in the range 2000 - 2060 keV, measured in the period August 1990 to May 2003 and November 1995 to May 2003, Fig. 19 the spectrum obtained with detectors 2,3,4,5 in the period Nov. 1995 - May 2003, and Fig. 20 the one measured in the same period with detectors 2,3,5.

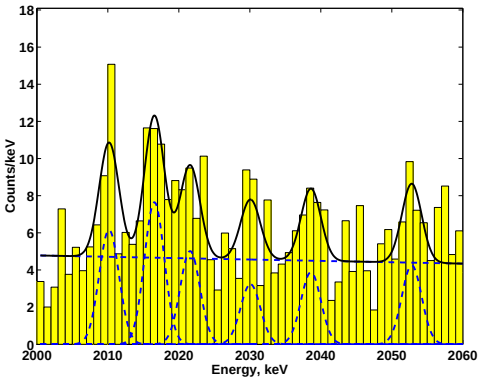

Fig. 20. Total spectrum in the range 2000 - 2060 keV obtained with detectors 2,3,5 (42.69 kg y) in the period November 1995 to May 2003, and its fit (see section 3.2).

3.1 Energy Calibration

Precise energy calibration for all detectors before summing the individual 2142 runs taken with the detectors, and finally summing the sum spectra of the different detectors (in total summing 9 570 data sets) is of extreme importance to achieve a good energy resolution of the total spectrum, (as seen in Figs. 15 - 20), and an optimum sensitivity of the experiment. A list of the energies of *all* identified lines (Figs. 15,16) is given in a recent paper [15], here we concentrate on the range of interest around $Q_{\beta\beta}$.

Table 4
Calibration of the weekly measured source spectra and of their sum, and the energy resolution and widths for the lines 1620.50, 2103.5 and 2614.53 keV over period 1995 - 2003.

Calibration period	Det. Nr.	E_γ line					
		^{212}Bi, ^{228}Th E_0=1620.50 keV [39]		SE ^{228}Th E_0=2103.5 keV [39]		^{228}Th E_0=2614.533 keV [39]	
		E_{peak} [keV]	FWHM [keV]	E_{peak} [keV]	FWHM [keV]	E_{peak} [keV]	FWHM [keV]
One of weekly spectra	1	1620.54	2.51	2103.36	3.65	2614.40	2.96
	2	1620.75	2.71	2103.58	3.85	2614.46	3.43
	3	1621.18	2.63	2103.35	3.65	2614.66	3.00
	4	1620.61	3.13	2103.49	4.47	2614.61	3.48
	5	1621.43	2.66	2103.59	3.82	2614.52	3.36
After summing over period 1995-2003	1	1620.90	2.60	2103.53	3.63	2614.52	3.00
	2	1620.65	2.99	2103.53	3.93	2614.53	3.40
	3	1621.63	2.75	2103.53	3.69	2614.52	3.04
	4	1620.78	3.66	2103.52	4.55	2614.53	3.98
	5	1621.29	2.87	2103.54	3.95	2614.54	3.38
After summing all 5 detectors over period 1995-2003							
		1621.12	3.02	2103.53	3.86	2614.53	3.27

Table 5
Calibration of background peaks in the measured sum spectrum for all five detectors, (period 1995 - 2003), and their determined widths.

Nuclide	E_0, keV	E_{peak} [keV]	FWHM [keV]
^{40}K	1460.83	1461.60	3.31
^{214}Bi	1764.495	1764.83	3.29
^{214}Bi	2204.21	2204.16	3.66
^{208}Tl	2614.533	2614.53	3.55

In this range for the calibration the lines at 2103.5 and 2614.5 keV were chosen (using a linear calibration), which reproduces the energies of other known lines in the high-energy part of the spectrum, around $Q_{\beta\beta}$ (see below and Tables 4÷5). Table 4 shows a slight broadening of the single escape (SE) peak at 2103.5 keV compared to the full-energy peak. This is a known effect, arising from the finite momentum of the electron-positron pair immediately before annihilation. Since this momentum causes one annihilation photon to have a slightly higher energy that its partner, in the case that only one photon is reabsorbed, the variation in the escaping energy leads to some broadening of the observed peak (see, e.g. [46]). The centroid of the single escape peak in a axial detector also can be slightly shifted to higher energies (on the order of 50 eV) as a result of effects due to the positron mobility in the detector. We think, however, that these tiny effects are not relevant in our case, and that having a calibration line very close in energy to $0\nu\beta\beta$ is the most important point in our case.

The stability of the experiment over the years and of the energy resolution and calibration is demonstrated in the following figures: Fig. 21 shows the sum of all weekly calibration spectra (366 spectra for each detector) for the 2614.5 keV Th line. Fig. 22 shows the resolution and energy position after summing the spectra of the five detectors ($\sim$ 1800 data sets). Table 4 gives the corresponding numbers.

The integrated resolution over 8 years of measurement is found to be 3.27 keV, i.e. better than in our earlier analysis of the data until May 2000 [1–3]. This is a consequence also of the refined summing procedure we used for the individual 9 570 data sets. The number achieved for 8 years of measurement is better than what another Ge experiment achieved in a shorter measurement of only 900 days [70].

Fig. 23 shows as another example the sum of all weekly calibration spectra for the 2103.5 keV line for each detector. The agreement of the energy positions of the different detectors is seen to be very good.

Fig. 24 shows the energies and widths obtained with the above calibration for some major background lines in the *measured total spectrum* during 1995

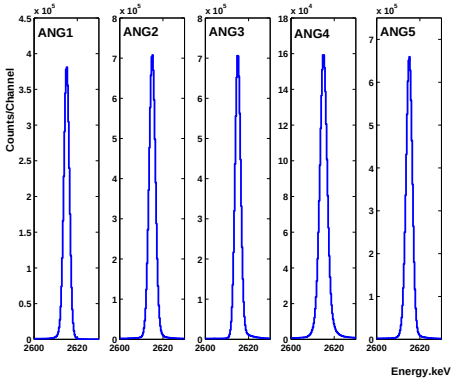

Fig. 21. *Sum* of the weekly calibration spectra for the 2614.5 keV of line ^{228}Th over the measuring time 1995 - 2003.

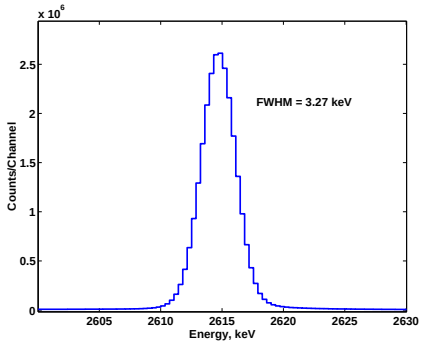

Fig. 22. Sum of the sum of the weekly calibration spectra of all five detectors shown in Fig. 21 (1830 spectra).

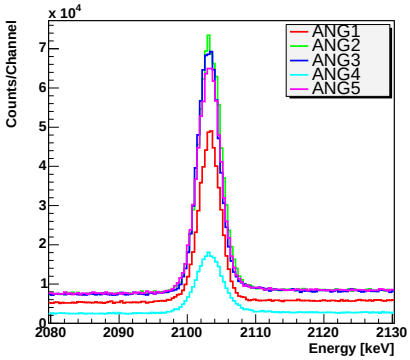

Fig. 23. Sum of calibration spectra for each detector (absolute intensities for the 2103.5 keV line for the period 1995 - 2003) (from top to bottom detectors: 2, 3, 5, 1, 4).

- 2003 (*no* source measurement), at 1460.8 keV (from ^{40}K), 1764.5 keV and 2204.2 keV (from ^{214}Bi), and 2614.5 keV (from ^{228}Th). Shown are the lines seen in the full spectrum, and in the spectrum of single site events (see section 4). The energies agree with the values given in the Table of Isotopes [39] (see Table 5).

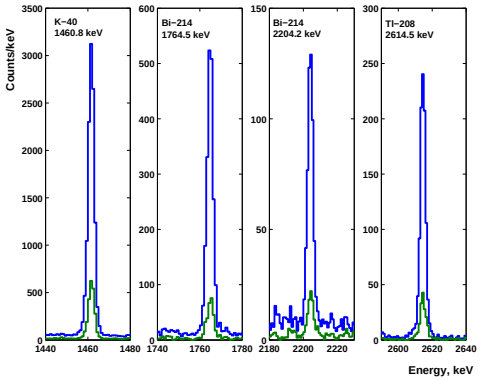

Fig. 24. Position and widths of some major background lines in the spectra measured in the period 1995-2003 (*no* source) determined with the calibration outlined above. Sum of all five detectors (i.e. of 9570 spectra). Blue line (peak at the top - full spectra, green (peak at bottom) - single site events) (see also Table 5).

Fig. 25 shows (taking as example detector Nr. 1) the distribution of the line maxima of the 2103.5 keV line in the 366 measured calibration spectra. The rms value of the deviation from the known value of the maximum is 0.36 channels, i.e. the line position can be determined (for a line of large intensity - here order of 500 events per individual line) with an order of precision of 0.13 keV. For a line with less statistics the rms value could range up to the order of a keV (see [9,19]).

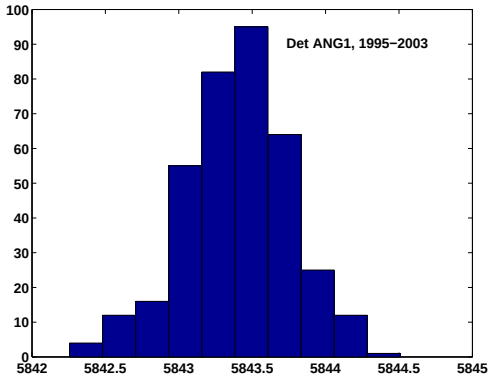

Fig. 25. Distribution of the line maxima of the 2103.5 keV line in 366 measured calibration spectra (for detector Nr. 1), as function of channel number.

Figs. 26, 27 show in detail the change in the positions (channel numbers) of some lines in the measured calibration spectra over the measuring time, e.g. by shift of gain or by change of amplification of the amplifiers, or microphonics, etc. and the situation after calibration of the weekly spectra, leading to the numbers given in Tables 4,5.

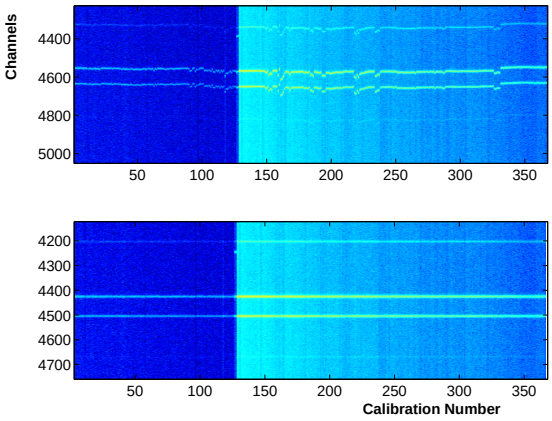

Fig. 26. Position of lines 1592.5 and 1620.5 keV in the calibration spectra over 8 years of measurement (1995 - 2003) in the HEIDELBERG-MOSCOW experiment, for detector number 1 (top), and position after calibration of the individual spectra (bottom).

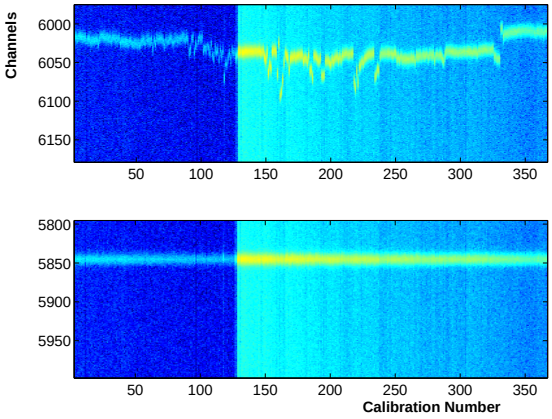

Fig. 27. Position of line 2103.5 keV in the calibration spectra over 8 years of measurement (1995 - 2003) in the HEIDELBERG-MOSCOW experiment for detector number 4 (top), and position after calibration of the individual spectra (bottom).

3.2 Analysis of the Spectra

In the measured spectra (Figs. 16 ÷ 20) we see in the range around $Q_{\beta\beta}$ the ^{214}Bi lines at 2010.7, 2016.7, 2021.8, 2052.9 keV, the line at $Q_{\beta\beta}$ and a candidate of a line at $\sim$ 2030 keV (see also [9,10]). The spectra have been analyzed by *different methods*: Least Squares Method, Maximum Likelihood Method (MLM) and Feldman-Cousins Method. The analysis is performed *without subtraction of any background*. We always process background-plus-signal data since the difference between two Poissonian variables does *not* produce a Poissonian distribution [48]. This point has to be stressed, since it is sometimes overlooked. So, e.g., in [79] a formula is developed making use of such subtraction and as a consequence the analysis given in [79] provides overestimated standard errors.

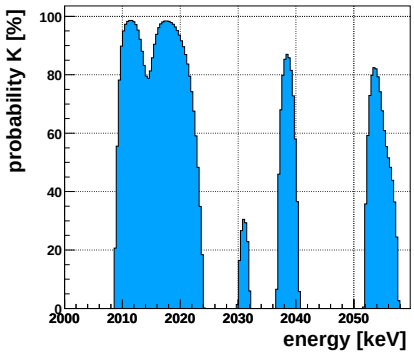

Fig. 28. Scan for lines in the full spectrum taken from 1995 - 2003 with detectors Nr. 1,2,3,4,5, (Fig. 18) with the MLM method (see text). The Bi lines at 2010.7, 2016.7, 2021.8 and 2052.9 keV are clearly seen, and in addition a signal at $\sim$ 2039 keV.

Fig. 28 shows, as example, the result of a peak-scanning procedure for the spectra shown in Fig. 18 performed with the MLM method. At each energy the program determines the probability to have a line with correct properties - Gaussian - shaped, with a width determined from neighboring background lines - assuming all the rest of the spectrum as background. This is a highly conservative assumption - in view of the lines seen in Figs. 17 $\div$ 20. This method projects out lines from the background, and earlier [1–3] was important to identify the weak background lines (from ^{214}Bi) around $Q_{\beta\beta}$, and also the line at $Q_{\beta\beta}$ (see also [9,19]), which now are also *directly* clearly seen in the spectra (Fig. 17 $\div$ 20).

We have performed first a simultaneous fit of the range 2000 - 2060 keV of the measured spectra by nonlinear least squares methods, using the Levenberg-Marquardt algorithm [49–51,47].

It was shown [55] that the least squares method is applicable in any statistics under the following conditions: 1) relative errors asymptotic to zero, 2) ratio of signal to background asymptotic constant. It does not require exact knowledge of the probability density function of the data. In any case we *followed the suggestion* of the Particle Data Group [53] to compare the number of events in the spectrum with the number of events in the fit. It was found that they were identical on a percent level, so that no normalization was needed.

We follow the standard procedure: we have a histogram N_i - corresponding to a spectrum with some binning E_i (for optimal binning see e.g. [55]), and i denoting the number of bin of our analysed spectra. We fit this spectrum using n Gaussians (n is equal to the number of lines, which we want to fit) $G(E_i, E_j, \sigma_j)$

$$G(E_i, E_j, \sigma_j) = \frac{1}{\sigma_j\sqrt{2\pi}} \exp\Big[-\frac{(E_i - E_j)^2}{2\sigma_j^2}\Big] \qquad (2)$$

and we use different background models $B(E_i)$: simulated background (linear with fixed slope) (see [15]), linear, and constant. The fitting function $F(E_i)$ is a sum of Gaussians and background:

$$F(E_i) = \sum_{j}^{n} S_j \times G(E_i, E_j, \sigma_j) + B(E_i) \tag{3}$$

Minimizing the norm of errors using the nonlinear least squares method with the Levenberg-Marquardt algorithm, the parameters are found as

$$S_j, E_j, \sigma_j, b = \arg\min \sum_i \left(F(E_i) - N(E_i)\right)^2, \tag{4}$$

where:

- n is the number of used Gaussians $G(E_i, E_j, \sigma_j)$, $j = 1..n$;
- E_j are the estimated centroid energies;
- σ_j are the estimated widths of Gaussians;
- S_j are the estimated peak intensities;
- b is background index;
- m is the number of bins in the spectrum, i=1, .., m;
- $B(E_i)$ denotes the background model;
- N_i denotes the number of counts in the bin corresponding to energy E_i.

Error estimate: the Levenberg-Marquardt method [50,52] is one of the most developed and tested minimization algorithm, finding fits most directly and efficiently [51]. It also is reasonably insensitive to the starting values of the parameters. This method has advantages over others of providing an estimate of the full error matrix. The MATLAB Statistical Toolbox [56] provides functions for confidence interval estimation for all parameters. It uses residual of fit and Jacobian matrix J_{ij} of F_i around the solution of eq. 4 to obtain estimates of the errors. Using the same method, but weighting the data, leads to a slight underestimation of the background in the fits of the spectra, but essentially to the same results.

We tested the confidence intervals calculated by the MATLAB statistical functions with numerical simulations. As done earlier for other statistical methods [2,3], we have simulated 100 000 spectra with Poisson-distributed background and a Gaussian-shaped (Poisson-distributed) line of given intensity, and have investigated, in how many cases we find in the analysis the known intensities inside the given confidence range. Table 6 shows that the confidence levels determined are correct within small errors. For example for a situation which we have in our experiment, a line of 30 counts on a background of 10 events per keV, we analysed 100 000 simulated spectra. In 99 979 cases we find the true value of the line intensity within the 4σ error interval. This means the confidence level calculated for such a line by this method is correct within $\sim 0.3\ \sigma$.

Table 6
Result of simulation of 100 000 (in each entry) spectra with Poisson-distributed background and a Gaussian-shaped line of given intensity for different background - B, and peak area - S, by the least squares method, using the Levenberg-Marquardt algorithm [50,51]. Given is the number of spectra where the true number of counts in the line is found in the calculated confidence area.

B	S = 10				S = 20				S = 30			
	1σ	2σ	3σ	4σ	1σ	2σ	3σ	4σ	1σ	2σ	3σ	4σ
2	66505	93781	99183	99932	63967	93176	99219	99952	62094	92191	99121	99932
7	66879	91683	98476	99900	67618	94733	99498	99961	66332	94443	99539	99967
10	64962	90029	98380	99918	68210	94921	99455	99933	67352	94784	99554	99979
Expected:												
	68269	95449	99730	99994	68269	95449	99730	99994	68269	95449	99730	99994

The second standard method, we have used to analyze the measured spectra, is the Maximum Likelihood Method (MLM) using the root package from CERN [57], which exploits the program MINUIT for error calculation. For this purpose the program provided there had to be extended for application to non-integer numbers (for details see [58]). We performed also in this case a test of the given confidence intervals given by this program, by numerical simulations. It has been found that the program systematically overestimates the errors, leading to too small confidence levels. For example for the case of 30 events in the line and a background of $\sim$10 events the method finds the true value in 99 971 spectra within the 3 σ confidence range. This means that the c.l. given by the method here is underestimated by 0.63σ. Taking this into account, the application of the MLM yields results for the confidence levels consistent with the Least Squares Method. By the way also the Bayesian method, as used in [1–3], was found to overestimate, on a similar level as the MLM, the errors, as indicated in Table 5 in [3]. As a consequence the confidence levels given in [1–3] were systematically too low (for details see [58]). The third method used for analysis is the Feldman-Cousins-Method (FCM) described in detail in [53,54].

4 Results

4.1 Full spectra

Figs. 17 $\div$ 20 show together with the measured spectra in the range around $Q_{\beta\beta}$ (2000 - 2060 keV), the fits using the first of the methods described in

section 3. In these fits a linear decreasing shape of the background as function of energy was chosen corresponding to the complete simulation of the background performed in [15] by GEANT4 (see Fig. 8).

In these fits the peak positions, widths and intensities are determined simultaneously, and also the *absolute* level of the background. E.g. in Fig. 18, the *fitted* background corresponds to (55.94 ± 3.92) kg y if extrapolated from the background *simulated* in [15] for the measurement with 49.59 kg y of statistics (see Fig. 8). This is almost *exactly* the statistical significance of the present experiment (56.66 kg y) and thus a very nice proof of consistency.

Table 7 gives the intensities of the lines for the full spectra obtained by the fits of the range 2000 - 2060 keV (Figs. 17 ÷ 20), and of the single site events spectrum shown in Fig. 31, assuming the linearly decreasing background as described. Assuming a *constant* background in the range 2000 - 2060 keV or keeping also the *slope* of a linearly varying background as a free parameter, yields very similar results.

Table 7
Results of the analysis of the measured spectra by non-linear optimization least squares fit of the range 2000-2060 keV. Given are energies and intensities resulting from the fit, and their 1σ errors.

Line	Full spectra						SSE spectrum	
	Fig. 17		Fig. 18		Fig. 19		Fig. 31	
	Detectors 1,2,3,4,5				Detectors 2,3,4,5		Detectors 2,3,4,5	
(keV)	1990-2003		1995-2003		1995-2003		1995-2003	
	71.7 kg y		56.66 kg y		51.39 kg y		51.39 kg y	
	Energy [keV]	Intensity [events]	Energy [keV]	Intensity [events]	Energy [keV]	Intensity [events]	Energy [keV]	Intensity [events]
2010.7	2009.89 ±0.32	39.85 ±6.89	2010.37 ±0.37	28.62 ±5.69	2010.10 ±0.37	27.41 ±5.44	2010.01 ±0.69	9.99 ±3.74
2016.7	2015.74 ±0.43	32.81 ±7.06	2016.25 ±0.43	27.73 ±5.89	2016.39 ±0.37	28.55 ±5.48	2016.21 ±1.48	4.68 ±3.74
2021.8	2019.94 ±0.54	26.06 ±7.06	2020.33 ±0.68	17.47 ±5.88	2021.02 ±0.57	18.63 ±5.47	2022.05 ±1.16	5.96 ±3.73
∼2030	2029.78 ±0.81	15.54 ±6.87	2030.07 ±0.72	14.52 ±5.67	2030.13 ± 0.63	15.76 ±5.42	2031.03 ±0.8	8.6 ±3.73
2039.0	2038.07 ±0.44	28.75 ±6.86	2038.44 ±0.45	23.04 ±5.66	2038.52 ±0.51	19.58 ±5.41	2037.56 ±0.56	12.36 ±3.72
2052.9	2053.18 ±0.37	33.88 ±6.84	2053.13 ±0.49	21.48 ±5.64	2053.03 ±0.48	20.68 ±5.40	2052.65 ±0.47	14.75 ±3.71

The signal at $Q_{\beta\beta}$ in the full spectrum at $\sim 2039\,\mathrm{keV}$ reaches a $4.2\,\sigma$ confidence level for the period 1990-2003, and of $4.1\,\sigma$ for the period 1995-2003. We have given a detailed comparison of the spectrum measured in this experiment with other Ge experiments in [9,19]. It is found that the most sensitive experiment with natural Ge detectors [11], and the first experiment using enriched (not yet high-purity) ^{76}Ge detectors [12] find essentially the same background lines (^{214}Bi etc.), but *no* indication for the line near $Q_{\beta\beta}$. This is consistent with the rates expected from the present experiment due to their lower sensitivity: $\sim$0.7 and $\sim$1.1 events, respectively. It is also consistent with the result of the IGEX ^{76}Ge experiment [13], which collected only a statistics of $8.8\,\mathrm{kg\,y}$, before finishing in 1999, and which should expect $\sim$2.6 events, which they might have missed. Their published half-life limit is overestimated as result of an arithmetic mistake (see [14]).

The fits obtained with the Maximum Likelihood Method agree with the results, given in Table 7. The estimations of the Feldman-Cousins Method yield confidence levels for the line at $Q_{\beta\beta}$ at a $\sim 4\sigma$ level. The uncertainty in the determination of the background here is larger, than in a consistent fit of the full range of interest by the other two methods.

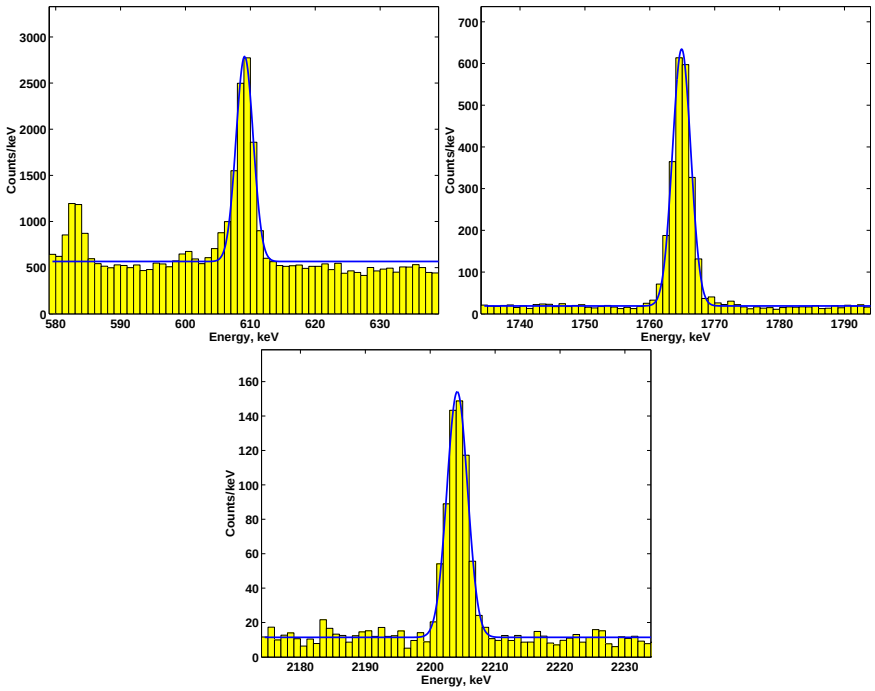

Fig. 29. The strong Bi lines at 609.31 (upper left), 1764.5 (upper right) and 2204.2 keV (bottom) measured with all five detectors in the period 1990 ÷ 2003.

We have compared the intensities of the weak Bi-lines near $Q_{\beta\beta}$ with the expectations from the strong lines at 609.31, 1764.5 and 2204.2 keV. The latter appear in the spectrum measured with all detectors in the period 1990 ÷ 2003 as shown in Fig. 29. From the measured intensities and our earlier GEANT4

simulations [15] we expect intensities for the lines at 2010.7, and 2016.7 keV, as observed within the error bars. For the lines at 2021.8 and 2052.9 keV somewhat larger intensities are found, which however, are still consistent within the 2.5σ error of the measurement.

4.2 Time structure of events

There are at present *no other* running experiments (with reasonable energy resolution) which can - not to speak about their lower sensitivity - *in principle* give *any further-going* information in the search for double beta decay than shown up to this point: namely a line at the correct energy $Q_{\beta\beta}$. Also most future projects cannot determine more. The HEIDELBERG-MOSCOW experiment developed some *additional tool* of potential independent verification, whose present status will be presented in this section. The method is to exploit the time structure of the events and to try to select $\beta\beta$ events by their pulse shape.

Coming to pulse shape analysis, our conclusions become model-dependent. We apply here first a method similar to that described earlier [3,4]. We accept only events as SSE, classified by one of the neuronal net methods, and in most cases simultaneously also by the second and third method mentioned in section 2, as SSE (for details see [58]). Two calibrations of the efficiency of this method have been performed in 2002 and September 2003, by using a ^{228}Th source in the detector chamber containing detectors 2,3,5, and in November 2003 for detector 4 (see section 2.2). They yield the result shown in Fig. 30. Taking all four detectors together, the SSE line at 1592.5 keV is reduced to 62%, the normal Thorium lines to ∼20%. (There is some variation of these values for the different detectors). Practically the same reduction of normal γ-line intensities is found for lines measured in our *spectrum* taken in the period 1995 - 2003, and also in another calibration measurement using a ^{226}Ra source (95.2 k Bq) inside the detector chambers yielding a lot of ^{214}Bi lines (see Fig. 30).

The SSE spectrum obtained by this method from the measurement over the period 1995 - 2003 is shown in Fig. 31 (compare to Fig. 19).

We find a 3.3σ signal for the line near $Q_{\beta\beta}$ and we find the other lines, at 2010.7, 2016.7 and 2021.8 keV to be consistent in intensity with normal γ-lines (see Fig. 30). In particular the E0 transition at 2016.7 keV, which should consist to 100% of multiple site events, since it is seen *only* by the True Coincidence Summing Effect of two successive γ-transitions (see [10]) is fully suppressed.

There is (see Fig. 31) some indication on a confidence level of $\sim 2\sigma$, of an

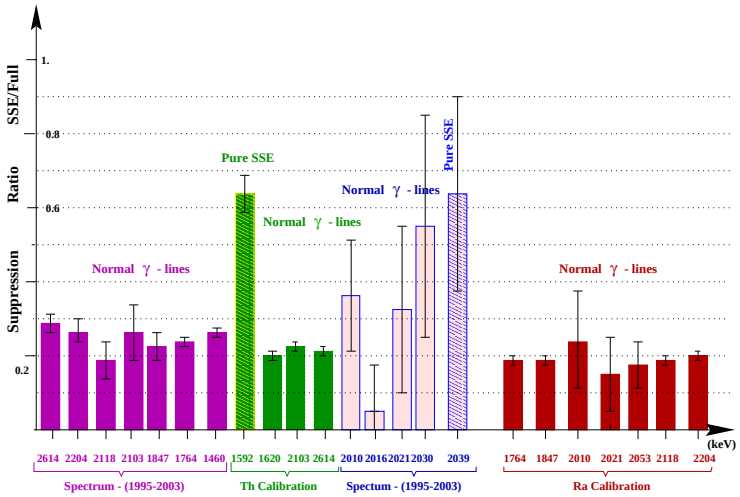

Fig. 30. Relative suppression ratios: Remaining intensity after pulse shape analysis compared to the intensity in the full spectrum. Result of a calibration measurement with a Th source. Compared to the known SSE line at 1592.5 keV, the intensities of the 2103.5 keV line (single escape peak, known to be 100% MSE) and the full energy peak at 2614.5 keV are strongly reduced (error bars are $\pm 1\sigma$). The same order of reduction is found for the Thorium lines and the strong Bi lines occuring in our spectrum, and in a calibration measurement with a ^{226}Ra source.

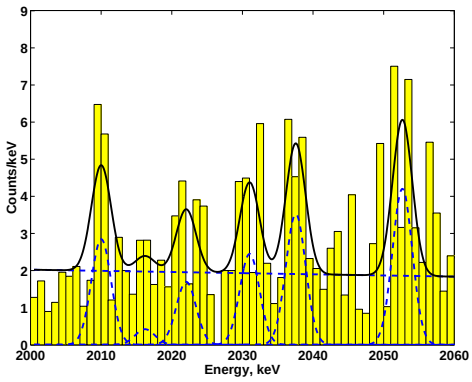

Fig. 31. The single site sum spectrum of the four detectors 2,3,4,5 for the period November 1995 to May 2003 (51.389 kg y), and its fit (see section 3), in the range 2000 - 2060 keV.

unidentified line around 2030 keV (see Table 7). This line might be understood as originating from electron conversion of the γ-line at 2118 keV originating from ^{214}Bi. The K shell binding energy in ^{214}Bi is 88 keV [39]. With a conversion probability of 0.3-1.% [40] and an efficiency for detection of a γ-line of $\sim$13%, as determined by a GEANT4 simulation for this energy of 2118 keV, and larger conversion coefficients and detection efficiencies for subsequent lower-energy transitions in this cascade, one could expect something in the order of $\sim$5-10 events from this line. On the other hand it was reported already in [9,19] that the structure at $\sim$ 2030 keV differs in energy from $Q_{\beta\beta}$ just by the K-shell X-ray energies of Ge(Se) of 9.2 (10.50) keV, or the K-shell

atomic binding energies of 11.10 (12.66) keV (see [39]).

That the PSA method, for the 1592.5 keV line, is functioning also in our *measured* spectrum, (*not* source spectrum) is seen in Fig. 32. In the full spectrum the 1592 keV line *is not* visible, but it is covered by the 1588.2 keV line from ^{228}Ac. It is however, growing out in the SSE spectrum (see Fig. 32), where the neighbouring line at 1588.2 keV from ^{228}Ac is strongly suppressed. At the same time the 1620 keV line from ^{228}Th is also found to be strongly suppressed.

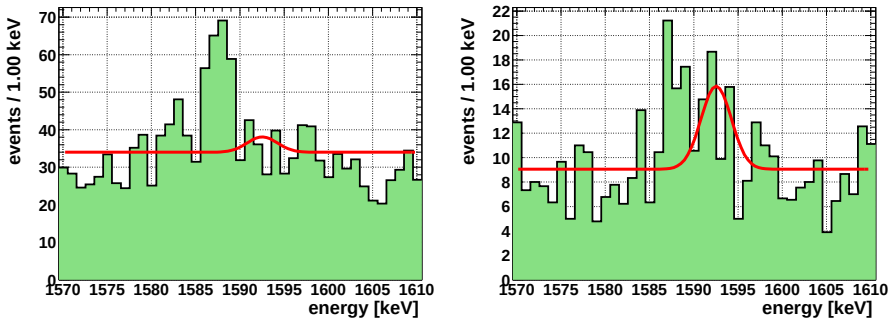

Fig. 32. Part of the spectrum measured with detectors 2,3,4,5 in the period 1995 - 2003 around the 1592.5 keV double escape line of the 2614.5 keV γ-line from ^{208}Tl. Left: full spectrum. Right: pulse-shape selected spectrum (see text). The red lines are shown to indicate the position of the 1592.5 keV line.

We would like to report, that we found an indication that a neuronal net method selection of the specific pulse shapes created by double beta decay could possibly still be done with much higher sensitivity. This is shown by Fig. 33. Here an empirically defined subclass of shapes selected by one of the

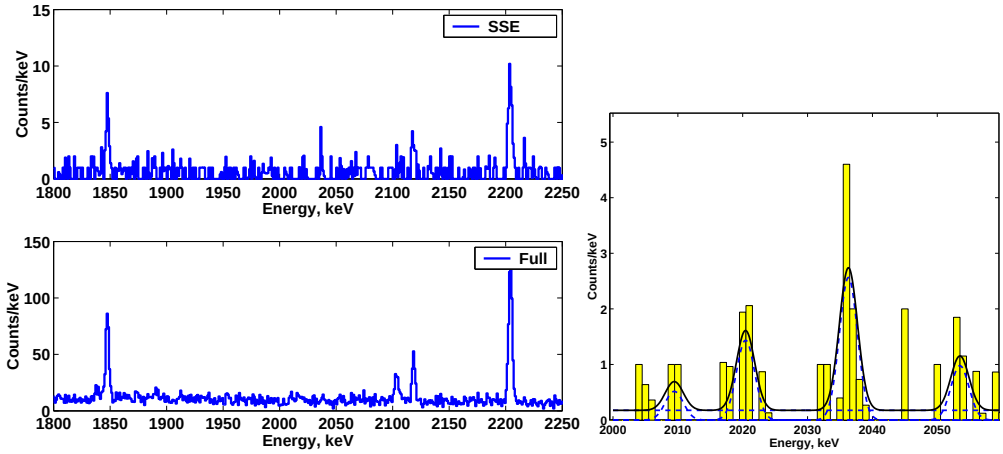

Fig. 33. Left top: The pulse shape selected spectrum (subclass of events selected in Fig. 31) measured with detectors 2,3,4,5 from 1995-2003, see text. Left bottom: The full spectrum measured with detectors 2,3,4,5 from 1995-2003. Right: As in left upper figure, but energy range 2000-206 keV.

above used neuronal net methods is selected. Except a line which sticks out

sharply near $Q_{\beta\beta}$, *all* other lines are very strongly suppressed. The probability to find ∼7 events in two neighboring channels from background fluctuations is calculated to be 0.013%. Thus, we see a line near $Q_{\beta\beta}$ at a 3.8σ level. Fig. 33 also shows the range 1800 - 2250 keV for the same selection, and the full spectrum in this range. The line near $Q_{\beta\beta}$ is standing out clearly. This method selects *part* of the events seen in Fig. 31, being at the same only weakly sensitive for the events in the 1592.5 keV double escape peak. This might indicate that indeed the pulse shapes of double beta events are somewhat different from pair creation events. This second method also fulfills the criterium to select properly the *continuous* $2\nu\beta\beta$ *spectrum* (which is *not* properly done by the first method (see Fig. 34).

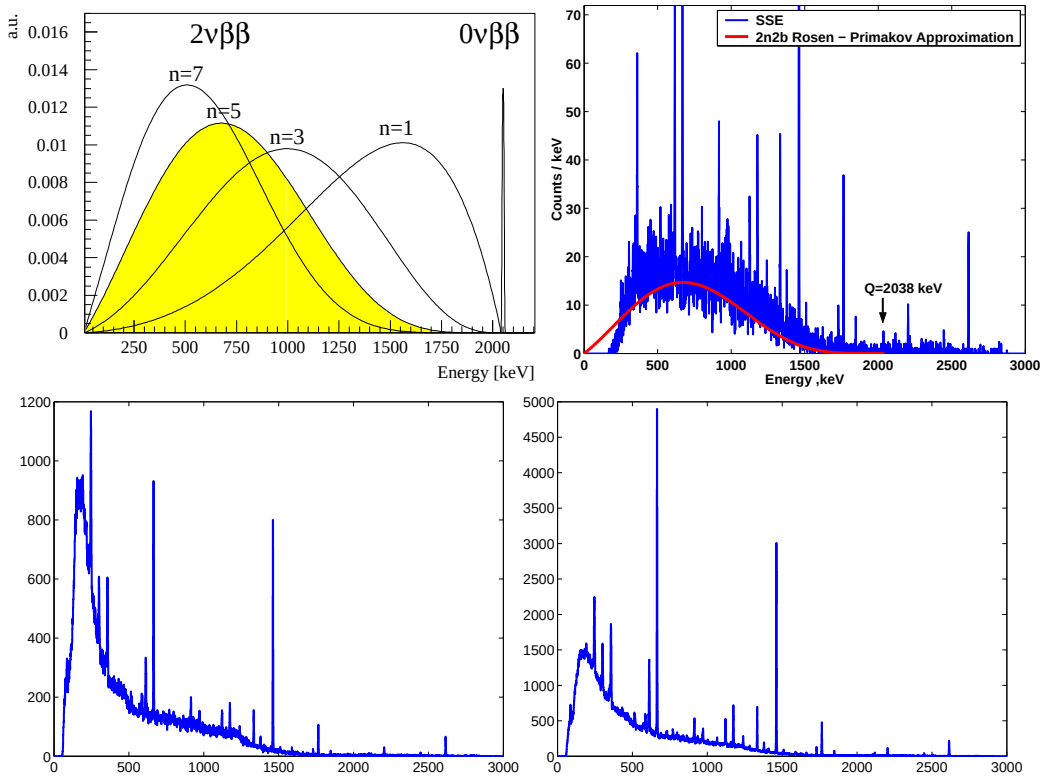

Fig. 34. Top panel: left. Sum energy spectra of the two emitted electrons for $0\nu\beta\beta$ and $2\nu\beta\beta$ (n=5), and for several hypothetical Majoron-accompanied double beta decay modes (n=1,3,7) (schematic). Right (top panel): the pulse-shape selected spectrum measured with detectors 2,3,4,5 from 1995÷2003 in the energy range of (100÷3000) keV, see text. Down panel: left. The spectrum selected as single site spectrum by the first method (see text). Right: The full spectrum mesured with detectors 2,3,4,5, from 1995÷2003.

The experimental signature of $2\nu\beta\beta$ decay is a continuous spectrum as shown in Fig. 34. The pulse shape spectrum selected with the second method, measured with detectors 2,3,4,5 from 1995÷2003 in the energy range of (100÷3000) keV, shows that this selected SSE events have a shape similar to the $2\nu\beta\beta$ spectrum. We consider this as an additional strong indication that

we really have observed neutrinoless double beta decay. Research is going on to come to more quantitative understanding [30].

The energy of this line determined by the spectroscopy ADC is slightly below $Q_{\beta\beta}$, but still within the statistical variation for a weak line (see [9,19]). In principle it is also understandable, that there must be some dependence of the energy determined by the ADC from the pulse shape (location of event in the detector, ballistic effects). Further investigations are needed to quantify this.

As pointed out already in section 2, a limitation of the presently used PSA methods (except for the second method discussed above), is in principle that they are calibrated with not precisely the same process, and, mainly at energies relatively far from $Q_{\beta\beta}$. Calibration conditions should be as close as possible to the conditions of the process to be investigated. Therefore, we plan to calibrate the neuronal net method *directly at the energy of* $Q_{\beta\beta}$. This could be done by measurements with an electron accelerator using electrons of ~ 1 MeV (this is a proposal by I. Bergström [108]), or with a source of monoenergetic conversion electrons of ~ 1 MeV, for example using ^{207}Bi *inside* the detector. This latter work is in progress. Fig. 35 shows the ^{207}Bi source of $\sim$50 Bq activity just put in form of a drop on the contact of a Ge detector.

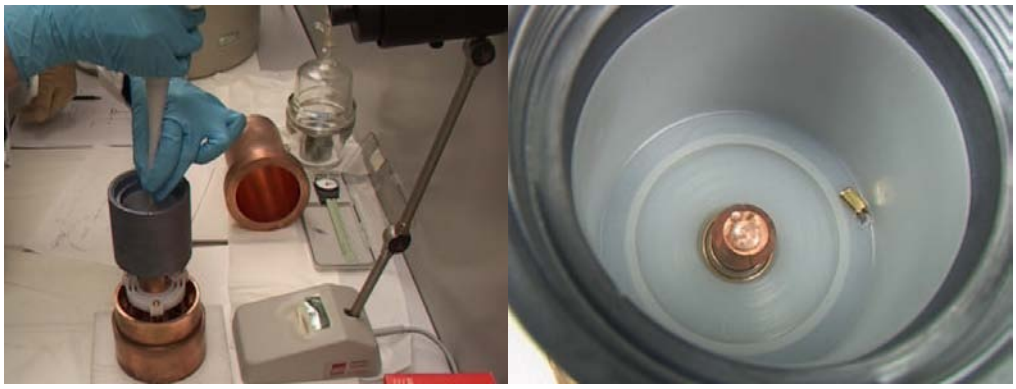

Fig. 35. Detector cup of a Ge detector (made of Si) and the copper contact inside, onto which a drop of a solution containing ^{207}Bi ($\sim$50 Bq of activity) has been positioned.

Concluding this section, the investigation of $\beta\beta$-like events is supporting a line near $Q_{\beta\beta}$ consisting of $0\nu\beta\beta$ events. Further research into simulation of double beta events, and their pulse shapes in a Ge detector and their identification by neuronal methods is, however, required.

The 2039 keV line as a single site events signal cannot be the double escape line of a γ-line whose full energy peak would be expected at 3061 keV where no indication of a line is found in the spectrum measured up to 8 MeV. Fig. 36 shows the relevant part of the high-energy spectrum. The same argument holds for the 2030 keV line candidate.

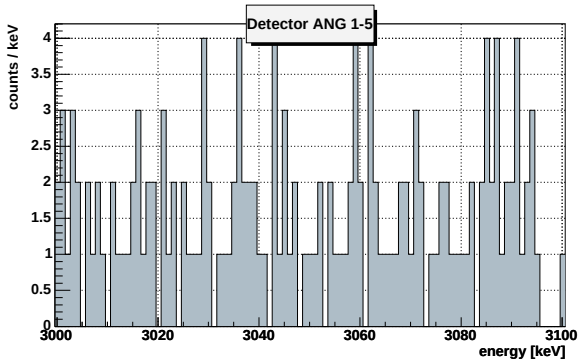

Fig. 36. High-energy part of the full spectrum, taken during the years 1995-2003.

5 Half-Life of Neutrinoless Double Beta Decay of ^{76}Ge

We have shown in chapter 4 that the signal at $Q_{\beta\beta}$ can be classified as consisting of single site events and with being not a γ line. The signal does not occur in the Ge experiments *not* enriched in the double beta emitter ^{76}Ge [11,9,19], while neighbouring background lines appear consistently in these experiments. On this basis we translate the observed number of events into the half-life for neutrinoless double beta decay. In Table 8 we give the half-lives deduced from the full data sets taken in the years 1995-2003 and in 1990-2003

Table 8
Half-life for the neutrinoless decay mode and deduced effective neutrino mass from the HEIDELBERG-MOSCOW experiment (the nuclear matrix element of [24] is used, see text). *) denotes best value.

Significance $[kg\,y]$	Detectors	$T^{0\nu}_{1/2}$ $[y]$ (3σ range)	$\langle m \rangle$ [eV] (3σ range)	Conf. level (σ)
Period 1990 ÷ 2003				
71.7	1,2,3,4,5	$(0.69 - 4.18) \times 10^{25}$ 1.19×10^{25}*	(0.24 - 0.58) 0.44*	4.2
Period 1995 ÷ 2003				
56.66	1,2,3,4,5	$(0.67 - 4.45) \times 10^{25}$ 1.17×10^{25}*	(0.23 - 0.59) 0.45*	4.1
51.39	2,3,4,5	$(0.68 - 7.3) \times 10^{25}$ 1.25×10^{25}*	(0.18 - 0.58) 0.43*	3.6
42.69	2,3,5	(2σ range) $(0.88 - 4.84) \times 10^{25}$ 1.5×10^{25}*	(2σ range) (0.22 - 0.51) 0.39*	2.9
51.39 (SSE)	2,3,4,5	$(1.04 - 20.38) \times 10^{25}$ 1.98×10^{25}*	(0.11 - 0.47) 0.34*	3.3

and of some partial data sets, including also the values deduced from the single site spectrum (Fig. 31). In this case we do conservatively not apply, from the reasons discussed in section 4, a calibration factor. The result is in this case a conservatively higher value for $T_{1/2}$ and smaller value for $\langle m \rangle$. Also given are

the effective neutrinos masses.

The result obtained is consistent with the limits given earlier from the HEIDELBERG-MOSCOW collaboration [8]. It is also consistent with the results we reported in [1–3,18,17,16].

Concluding we confirm, with 4.2σ (99.9973% c.l.) probability, our claim from 2001 [1–3,18,17,16] of first evidence for the neutrinoless double beta decay mode.

6 Consequences

As a consequence, at this confidence level, lepton number is not conserved. Further our result implies that the neutrino is a Majorana particle see, e.g. [72–74]. Both of these conclusions are *independent of any* discussion of nuclear matrix elements. The matrix element enters when we derive a *value* for the effective neutrino mass - making the probably *most natural assumption* that the $0\nu\beta\beta$ decay amplitude is dominated by exchange of a massive Majorana neutrino. The half-life for the neutrinoless decay mode is under this assumption given by [24,25]

$$[T^{0\nu}_{1/2}(0^+_i \to 0^+_f)]^{-1} = C_{mm}\frac{\langle m\rangle^2}{m_e^2} + C_{\eta\eta}\langle\eta\rangle^2 + C_{\lambda\lambda}\langle\lambda\rangle^2 + C_{m\eta}\langle\eta\rangle\frac{\langle m\rangle}{m_e} \qquad (5)$$
$$+C_{m\lambda}\langle\lambda\rangle\frac{\langle m\rangle}{m_e} + C_{\eta\lambda}\langle\eta\rangle\langle\lambda\rangle,$$

$$\langle m\rangle = |m^{(1)}_{ee}| + e^{i\phi_2}|m^{(2)}_{ee}| + e^{i\phi_3}|m^{(3)}_{ee}|\ , \qquad (6)$$

where $m^{(i)}_{ee} \equiv |m^{(i)}_{ee}|\exp(i\phi_i)$ $(i = 1, 2, 3)$ are the contributions to the effective mass $\langle m\rangle$ from individual mass eigenstates, with ϕ_i denoting relative Majorana phases connected with CP violation, and $C_{mm}, C_{\eta\eta}, ...$ denote nuclear matrix elements squared, which can be calculated, (see, e.g. [24], for a review and some recent discussions see e.g. [75,33,67,68,78,76,77,71]). Ignoring contributions from right-handed weak currents on the right-hand side of eq. (5), only the first term remains.

Using the nuclear matrix element from [24,25], we conclude from the half-life given above the effective mass $\langle m\rangle$ to be $\langle m\rangle = (0.2 \div 0.6)\,\mathrm{eV}$ (99.73% c.l.), with best value of $\sim 0.4\,\mathrm{eV}$.

The effective mass is closely related to the parameters of neutrino oscillation experiments, as can be seen from the following expressions

$$|m^{(1)}_{ee}| = |U_{e1}|^2 m_1,$$

$$|m_{ee}^{(2)}| = |U_{e2}|^2 \sqrt{\Delta m_{21}^2 + m_1^2},$$

$$|m_{ee}^{(3)}| = |U_{e3}|^2 \sqrt{\Delta m_{32}^2 + \Delta m_{21}^2 + m_1^2}.$$

Here, U_{ei} are entries of the neutrino mixing matrix, and $\Delta m_{ij}^2 = |m_i^2 - m_j^2|$, with m_i denoting neutrino mass eigenstates. U_{ei} and Δm^2 can be determined from neutrino oscillation experiments.

The matrix element given by [24] was the *prediction closest to* the *later* measured $2\nu\beta\beta$ decay half-life of $(1.74^{+0.18}_{-0.16}) \times 10^{21}$ y [15,6]. It underestimates the 2ν matrix elements by 32% and thus these calculations will also underestimate (to a smaller extent) the matrix element for $0\nu\beta\beta$ decay, and consequently correspondingly overestimate the (effective) neutrino mass. Allowing conservatively for an uncertainty of the nuclear matrix element of $\pm$ 50% (for discussions of the status of nuclear matrix elements we refer to [3,18,17,16]), the range for the effective mass may widen to $\langle m \rangle$ = (0.1 - 0.9) eV (99.73% c.l.).

Assuming other mechanisms to dominate the $0\nu\beta\beta$ decay amplitude, which has been studied extensively in recent years, the result allows to set stringent limits on parameters of SUSY models, leptoquarks, compositeness, masses of heavy neutrinos, the right-handed W boson and possible violation of Lorentz invariance and equivalence principle in the neutrino sector. For a discussion and for references we refer to [33,35,36,38].

With the value deduced for the effective neutrino mass, the HEIDELBERG-MOSCOW experiment excludes several of the neutrino mass scenarios allowed from present neutrino oscillation experiments (see Fig. 1, in [96]) - allowing only for degenerate mass scenarios [32,96].

We have shown in [3,9,19], that indirect support for the observed evidence for neutrinoless double beta decay evidence comes from analysis of other Ge double beta experiments (though they are unfortunately by far less sensitive, they yield independent information on the background in the region of the expected signal [9,10,19,20]).

The evidence for neutrinoless double beta decay is supported by various other recent experimental and theoretical results (see Table 8). Assuming the degenerate scenarios to be realized in nature we fix - according to the formulae derived in [31] - the common mass eigenvalue of the degenerate neutrinos to m = (0.1 - 3.5) eV. Part of the upper range is excluded by tritium experiments, which give a limit of m $<$ (2.3 - 2.8) eV (95% c.l.) [83]. The full range may only partly be checked by future tritium decay experiments [83] if at all [110].

The results from solar and atmospheric neutrino oscillations already yield, assuming degenerate neutrinos, a lower limit of the common mass eigenvalue

Table 9
Recent support of the neutrino mass deduced from $0\nu\beta\beta$ decay [1–3,10,9] by other experiments, and by theoretical work.

Experiment	References	m_ν (degenerate ν's)(eV)
$0\nu\beta\beta$	[1–3,10,9]	0.05 - 3.2
WMAP	[94,97]	< 0.23, or 0.33, or 0.50
CMB	[93]	< 0.7
CMB+LSS+X-ray gal. Clust.	[98]	$\sim$0.2 eV
SDSS+WMAP	[111]	< 0.57
Z - burst	[89,90]	0.08 - 1.3
g-2	[85]	> 0.2
Tritium	[83]	$<$2.2 - 2.8
ν oscillation	[91,92]	> 0.04
Theory:		
A_4-symmetry	[86]	> 0.2
identical quark and ν mixing at GUT scale	[88]	> 0.1
Alternative cosmological 'concordance model'	[100]	order of eV

of $> 0.04\,\mathrm{keV}$ [96,99].

Recently improved information has come from investigation of the cosmic microwave radiation, and from Large Scale Structure observations [94,97,98,111].

For WMAP a limit on the total neutrino masses of

$$m_s = \sum m_i < 0.69 \text{ eV} \qquad \text{at } 95\% \text{ c.l.}, \tag{7}$$

is given by the analysis of ref. [94]. It has been shown, however, that this limit may not be very realistic [97]. The latter shows that this limit on the total mass should be

$$m_s = \sum m_i < 1.0 \text{ eV} \qquad \text{at } 95\% \text{ c.l.} \tag{8}$$

The latter analysis also shows, that four generations of neutrinos are still allowed and in the case of four generations the limit on the total mass is increased to 1.38 eV, i.e. the common mass eigenvalue would be $0.46\,\mathrm{eV}$. If there is a fourth neutrino with very small mass, then the limit on the total mass of the three neutrinos is even further weakened. In Fig. 1 (of [96]) we show the contour line for WMAP assuming $\sum m_i < 1.0$ eV.

An analysis of CMB, large scale structure and X-rays from clusters of galaxies yields a 'preferred' value for $\sum m_\nu$ of $0.6\,\mathrm{eV}$ [98].

An analysis of SDSS+WMAP yields $\sum m_\nu \ < 1.7\,\mathrm{eV}$ [111].

Comparison of the WMAP results with the effective mass from double beta decay rules out completely (see [95,96]) a 15 years old old-fashioned nuclear matrix element of double beta decay, used in another analysis of WMAP [82]. In that calculation of the nuclear matrix element there was not included a realistic nucleon-nucleon interaction, which has been included by all other calculations of the nuclear matrix elements over the last 15 years.

As mentioned already in [21], the results from double beta decay and WMAP *together* may indicate that the neutrino mass eigenvalues have indeed the same CP parity, as required by the model of [88].

The range of $\langle m \rangle$ fixed in this work is, already now, in the range to be explored by the satellite experiments MAP and PLANCK [31,94,97]. The limitations of the information from WMAP, in particular the missing power to discriminate between different mass scenarios, are seen in Fig. 1 of [96] (see also in [3,32]), thus results of PLANCK are eagerly awaited.

The deduced best value for the mass is consistent with expectations from experimental $\mu \ \rightarrow \ e\gamma$ branching limits in models assuming the generating mechanism for the neutrino mass to be also responsible for the recent indication for an anomalous magnetic moment of the muon [85]. It lies in a range of interest also for Z-burst models recently discussed as explanation for super-high energy cosmic ray events beyond the GKZ-cutoff [89,90] and requiring neutrino masses in the range of 0.4 and (0.08 - 1.3) eV, respectively. A recent model with underlying A_4 symmetry for the neutrino mixing matrix also leads to degenerate neutrino masses > 0.2 eV, consistent with the present result from $0\nu\beta\beta$ decay [87,86]. The result is further consistent with the theoretical paper of [88]. Starting with the hypothesis that quark and lepton mixing are identical at or near the GUT scale, Mohapatra et al. [88] show that the large solar and atmospheric neutrino mixing angles can be understood purely as result of renormalization group evolution, if neutrino masses are quasi-degenerate (with *same* CP parity). The common Majorana neutrino mass then must be, in this model, larger than 0.1 eV. A Majorana nature of the neutrino is also concluded in the theoretical approach of [112].

The neutrino mass deduced leads to $0.002 > \sim \Omega_\nu h^2 < \sim 0.1$ and thus may allow neutrinos to still play an important role as hot dark matter in the Universe [37]. It could provide, what is required in a recent alternative cosmological 'concordance model' [100], based on an Einstein-de Sitter universe with *zero* cosmological constant, but requiring relic neutrinos with mass of order of eV.

7 Conclusion - Perspectives

Evidence for a signal at $Q_{\beta\beta}$ on a confidence level of 4σ has been observed confirming our earlier claim. On the basis of our understanding can be interpreted as evidence for neutrinoless double beta decay of ^{76}Ge, and for *total* lepton number nonconservation, and for a non-vanishing Majorana neutrino mass. Recent information from many *independent* sides seems to condense now to a nonvanishing neutrino mass of the order of the value found by the HEIDELBERG-MOSCOW experiment. This is the case for the results from CMB, LSS, SDSS, neutrino oscillations, tritium beta decay, particle theory and cosmology. An analysis of CMB, large scale structure and X-ray from clusters of galaxies yields a 'preferred' value for $\sum m_\nu$ of 0.6 eV [98]. The recent alternative cosmological concordance model requires relic neutrinos with mass of order of eV.

The importance of this first evidence for violation of *total* lepton number and of the Majorana nature of neutrinos for particle physics and cosmology is obvious. It requires beyond Standard Model Physics. It has been discussed that the Majorana nature of the neutrino tells us that spacetime does realize a construct that is central to construction of supersymmetric theories [60]. The lepton number violation observed will have also implications for the Early Universe.

From future projects to improve the present accuracy of the effective neutrino mass one has to require that they should be able to differentiate between a β and a γ signal, or that the tracks of the emitted electrons should be measured. At the same time, as is visible from the present information, the energy resolution should be *at least* in the order of that of Ge semiconductor detectors, or better. These requirements exclude at present calorimeter experiments like CUORE, CUORICINO, which *cannot* differentiate between a β and γ signal, etc, but also experiments like EXO [109], *if* the latter will not be able to reconstruct the tracks of the electrons, as it seems at present. An in principle very nice approach is the NEMO project, which *can* see tracks, but unfortunately has at present only a small efficiency, and a low energy resolution of more than 200 keV. The most sensitive future project, is probably the GENIUS project, proposed already in 1997 [101–103,34,33,35]. GENIUS seems to be the only of the new projects which simultaneously with its sensitivity for $0\nu\beta\beta$ decay has a huge potential for cold dark matter search, and for real-time detection of low-energy neutrinos (see [105–107,34,35,101,17,36,33,16]).

However, the necessity of GENIUS has been may be overcome by the historical development. The special potential of GENIUS for solar neutrinos was to look with large sensitivity to the LOW solution of the solar neutrino flux. Since KAMLAND [91] it seems now, however, to be clear, that the LMA so-

lution is realized in nature. Concerning cold dark matter, there is now a 6.4σ signal from DAMA [104]. This could hopefully be checked already, exploting the modulation signal, by the small GENIUS Test Facility, which has started operation with 10 kg of natural Germanium detectors in liquid nitrogen in Gran-Sasso on May 5, 2003 [22,23]. Before this experiment has not been completed, it is not clear, whether we need the full GENIUS for dark matter. The extreme sensitivity of GENIUS for $0\nu\beta\beta$ decay search was required at a time, where there was no evidence of a $0\nu\beta\beta$ signal. At present we have, however, a 4σ signal with a Ge experiment.

So, if one wants to get *independent* evidence for the neutrinoless double beta decay mode, one would probably wish to see the effect in *another* isotope, which would then simultaneously give additional information also on the nuclear matrix elements. In view of the above remarks, future efforts to obtain *deeper* information on the process of neutrinoless double beta decay, would require *a new experimental approach, different from all, what is at present persued.*

8 Acknowledgement:

The authors would like to thank all colleagues, who have contributed to the experiment over the last 15 years. They are particularly grateful to C. Tomei for her help in the early calibration of the pulse shape methods with the Th source and to Mr. H. Strecker for his constant technical support. Our thanks extend also to the technical staff of the Max-Planck Institut für Kernphysik and of the Gran Sasso Underground Laboratory. We acknowledge the invaluable support from BMBF and DFG, and LNGS of this project. We are grateful to the former State Committee of Atomic Energy of the USSR for providing the enriched material used in this experiment.

References

[1] H.V. Klapdor-Kleingrothaus et al. hep-ph/0201231 and Mod. Phys. Lett. A 16 (2001) 2409-2420.

[2] H.V. Klapdor-Kleingrothaus, A. Dietz, I.V. Krivosheina, Part. and Nucl. 110 (2002) 57-79.

[3] H.V. Klapdor-Kleingrothaus, A. Dietz, I.V. Krivosheina, Foundations of Physics 31 (2002) 1181-1223 and Corrigenda, 2003 home-page: http://www.mpi-hd.mpg.de/non_acc/main_results.html.

[4] H.V. Klapdor-Kleingrothaus, A. Dietz, I.V. Krivosheina, hep-ph/0302248 and in Proc. of DARK2002, 4th International Heidelberg Conference on Dark Matter in Astro and Particle Physics, Cape Town, South Africa, 4-9 Feb 2002, Springer, Heidelberg (2002), eds. by H.V. Klapdor-Kleingrothaus, R.D. Viollier, 404-411.

[5] H.V. Klapdor-Kleingrothaus, Proposal, MPI-1987-V17, September 1987.

[6] HEIDELBERG-MOSCOW Coll., Phys. Rev. D 55 (1997) 54.

[7] HEIDELBERG-MOSCOW Coll., Phys. Lett. B 407 (1997) 219-224.

[8] H.V. Klapdor-Kleingrothaus et al., (HEIDELBERG-MOSCOW Coll.), Eur. Phys. J. A 12, 147 (2001) and hep-ph/0103062, Proceedings, Third International Conference on Dark Matter in Astro- and Particle Physics, DARK2000 H.V. Klapdor-Kleingrothaus, ed., (Springer, Heidelberg, 2001) pp. 520-533.

[9] H.V. Klapdor-Kleingrothaus, A. Dietz, I.V. Krivosheina, Ch. Dörr, C. Tomei, Nuclear Instruments and Methods in Physics Research 510 A (2003) 281-289 and hep-ph/0308275.

[10] H.V. Klapdor-Kleingrothaus, O. Chkvorez, I. V. Krivosheina, C. Tomei, Nuclear Instruments and Methods in Physics Research 511 A (2003) 335-340 and hep-ph/0309157.

[11] D. Caldwell, J. Phys. G 17 (1991) S137-S144.

[12] A.A. Vasenko et al., Mod. Phys. Lett. A 5 (1990) 1299, and I. Kirpichnikov, Preprint ITEP (1991).

[13] C.E. Aalseth et al., Phys. Rev. D 65 (2002) 092007.

[14] H.V. Klapdor-Kleingrothaus, A. Dietz, I.V. Krivosheina, Phys. Rev. D, 2004, in press.

[15] Ch. Dörr, H.V. Klapdor-Kleingrothaus, Nuclear Instruments and Methods in Physics Research 513 A (2003) 596-621.

[16] H.V. Klapdor-Kleingrothaus, In Proc. of International Conf. SUGRA20, Boston, USA, 17-20 March, 2003, eds. by P. Nath, Rinton Press, Paramus, USA, 2003.

[17] H.V. Klapdor-Kleingrothaus, In Proc. of International Conf. NOON03, Kanazawa, February 2003, World Scientific, 2003, eds. Y. Suzuki and hep-ph/0307330.

[18] H.V. Klapdor-Kleingrothaus, In Proc. of International Conf. "Neutrinos and Implications for Physics Beyond the Standard Model", Stony Brook, USA, 11-13 October, 2002, ed. R. Shrock, World Scientific, 2003, 367-382 and hep-ph/0303217.

[19] H.V. Klapdor-Kleingrothaus et al., Phys. Lett. B 578 (2004) 54.

[20] H.V. Klapdor-Kleingrothaus, A. Dietz, I. Krivosheina, submit. to Phys. Rev. D.

[21] H.V. Klapdor-Kleingrothaus, in Proc. of International Conf. on Particle Physics Beyond the Standard Model, BEYOND02, Oulu, Finland June 2002, IOP, Bristol 2003, ed. H.V. Klapdor-Kleingrothaus, pp. 215-240.

[22] H.V. Klapdor-Kleingrothaus, O. Chkvorez, I.V. Krivosheina, H. Strecker, C. Tomei, Nuclear Instruments and Methods in Physics Research A 511 (2003) 341-346 and hep-ph/0309170.

[23] C. Tomei, A. Dietz, I. Krivosheina, H.V. Klapdor-Kleingrothaus, Nuclear Instruments and Methods in Physics Research A 508 (2003) 343-352, and hep-ph/0306257.

[24] A. Staudt, K. Muto, H.V. Klapdor-Kleingrothaus, Eur. Lett. 13 (1990) 31.

[25] K. Muto, E. Bender, H.V. Klapdor, Z. Phys. A 334 (1989) 177-186.

[26] J. Hellmig, H.V. Klapdor-Kleingrothaus, Nucl. Instrum. Meth. A 455 (2000) 638-644.

[27] J. Hellmig, F. Petry, H.V. Klapdor-Kleingrothaus, Patent DE19721323A.

[28] B. Majorovits, H.V. Klapdor-Kleingrothaus. Eur. Phys. J. A6 (1999) 463.

[29] (a) B. Maier, Dissertation, November 1995, MPI-Heidelberg; (b) F. Petry, Dissertation, November 1995, MPI-Heidelberg; (c) J. Hellmig, Dissertation, November 1996, MPI-Heidelberg; (d) B. Majorovits, Dissertation, December 2000, MPI-Heidelberg; (e) A. Dietz, Dipl. Thesis, Univ. Heidelberg, 2000 (unpublished), and Dissertation, June 2003, MPI-Heidelberg; (f) Ch. Dörr, Dipl. Thesis, Univ. Heidelberg, 2002 (unpublished).

[30] H.V. Klapdor-Kleingrothaus et al., in preparation.

[31] H.V. Klapdor-Kleingrothaus, H. Päs, A.Yu. Smirnov, Phys. Rev. D 63 (2001) 073005 and hep-ph/0003219; in Proc. of DARK'2000, Heidelberg, 10-15 July, 2000, Germany, ed. H.V. Klapdor-Kleingrothaus, Springer, Heidelberg (2001) 420-434.

[32] H.V. Klapdor-Kleingrothaus, U. Sarkar, Mod. Phys. Lett. A 16 (2001) 2469-2482.

[33] H.V. Klapdor-Kleingrothaus, "60 Years of Double Beta Decay - From Nuclear Physics to Beyond the Standard Model", World Scientific, Singapore (2001) 1281 pages.

[34] H.V. Klapdor-Kleingrothaus, Int. J. Mod. Phys. A 13 (1998) 3953.

[35] H.V. Klapdor-Kleingrothaus, Int. J. Mod. Phys. A 13 (1998) 3953 and in Proc. of Int. Symposium on Lepton and Baryon Number Violation, Trento, Italy, 20-25 April, 1998, ed. H.V. Klapdor-Kleingrothaus and I.V. Krivosheina, IOP, Bristol, (1999) 251-301 and Preprint: hep-ex/9901021.

[36] H.V. Klapdor-Kleingrothaus, Springer Tracts in Modern Physics, 163 (2000) 69-104, Springer-Verlag, Heidelberg, Germany (2000).

[37] H.V. Klapdor-Kleingrothaus, Int. J. Mod. Phys. A 17 (2002) 3421-3431, and in Proc. of Intern. Conf. LP01, WS 2002, Rome, Italy, July 2001.

[38] H.V. Klapdor-Kleingrothaus, U. Sarkar, hep-ph/0302237.

[39] R.B. Firestone, V.S. Shirley, Table of Isotopes, 8th Ed., John W.& Sons Inc., N.Y. (1998) and National Nuclear Data Center, brookhaven national Laboratory, Evaluated Nuclear Structure Data File (ENSDF), http://www.nndc.bnl.gov/nndc/ensdf/

[40] K. Siegbahn, "Alpha-, beta- and Gamma-Ray Spectroscopy", vol. 1, 2, 4th printing (1974), North-Holland Publ. Company, Amsterdam.

[41] G. Douysset et al., Phys. Rev. Lett. 86 (2001) 4259 - 4262, and I. Bergström et al., in Proc. of Intern. Conf. on Particle Physics Beyond the Standard Model, BEYOND'02, Oulu, Finland June 2002, IOP, Bristol and Philadelphia, UK, (2003) 197 p., ed. H.V. Klapdor-Kleingrothaus and in BEYOND 2003, Castle Ringberg, Germany, 10 - 14 June, 2003, Springer, Heidelberg, 2004, ed. H.V. Klapdor-Kleingrothaus.

[42] J.G. Hykawy et al., Phys. Rev. Lett. 67 (1991) 1708.

[43] G. Audi, A.H. Wapstra, Nucl. Phys. A 595 (1995) 409-480.

[44] R.J. Ellis et al., Nucl. Phys. A 435 (1985) 34-42.

[45] AMETEK (ORTEC) Co., private communication.

[46] G.F. Knoll, "Radiation Detection and Measurement", second ed. 1989, John Wiley & Sons.

[47] J.C. Lagarias, J.A. Reeds, M.N. Wright, P.E. Wright, "Convergence Properties of the Nelder-Mead Simplex Method in Low Dimensions", *SIAM Journal of Optimization* 9, Nr. 1 (1998) 112-147.

[48] M.D. Hannam, W.J. Thompson, Nucl. Instr. Meth. A 431 (1999) 239-251.

[49] Ch.L. Lawson, R.J. Hanson, "Solving Least Square Problems", SIAM, Classics in Applied Mathematics, 1995.

[50] D.W. Marquardt, J. Soc. Industr. Appl. Math. 11 (1963) 431-441.

[51] Ph.R. Bevington, D.K. Robinson, "Data Reduction and Error Analysis for the Physical Sciences", (1992), McGraw-Hill, Inc., New York, second edition, 328 p.

[52] T.H. Martin, B.M. Mohammad, IEE Trans. Neural Networks, vol. 5, pp. 959-963, November 1996.

[53] D.E Groom et al., Particle Data Group, Eur. Phys. J. C 15 (2000) 1.

[54] G.J. Feldman, R.D. Cousins, Phys. Rev. D 57 (1998) 3873.

[55] V.B. Zlokazov, preprint JINR-P10-86-502, Sep. 1986 and JINR-P10-88-94, Mar. 1988, Dubna, JINR, Russia.

[56] www.mathworks.com

[57] http://root.cern.ch/root/html/

[58] H.V. Klapdor-Kleingrothaus et al., in preparation.

[59] E. der Mateosian, M. Goldhaber, Phys. Rev. 146 (1966) 810-815.

[60] D.V. Ahluwalia, in Proc. of Physics Beyond the Standard Model: Beyond the Desert 02, BEYOND'02, Oulu, Finland, 2-7 Juni, 2002, IOP, Bristol, 2003, ed. H.V. Klapdor-Kleingrothaus, 143-160; D.V. Ahluwalia, M. Kirchbach, Phys. lett. B 529 (2002) 124.

[61] R. Davis Jr., Phys. Rev. 97 (1995) 766-769.

[62] E.N. Alekseev, L.N. Alekseeva, V.I. Volchenko, I.V. Krivosheina, JETP Lett. 45 (1987) 589-592, Pisma Zh. Eksp. Teor. Fiz. 45 (1987) 461-464; E.N. Alekseev, L.N. Alekseeva, I.V. Krivosheina, V.I. Volchenko, Phys. Lett. B 205 (1988) 209-214; E.N. Alekseev et al., JETP Lett. 49 (1989) 548-552, Pisma Zh.Eksp.Teor.Fiz. 49 (1989) 480-483; Sov. Phys. JETP 72 (1991) 585-589, Zh. Eksp. Teor. Fiz. 99 (1991) 1057-1065.

[63] K.S. Hirata et al., Phys. Rev. Lett. 58 (1987) 1490.

[64] R.M. Bionta et al., Phys. Rev. Lett. 58 (1987) 1494.

[65] Y. Fukuda et al. (Super-Kamiokande Collaboration), Phys. Lett. B 467 (1999) 185-193.

[66] GNO Collaboration, Nucl. Phys. Proc. Suppl. 110 (2002) 311-314; Dzh.N. Abdurashitov et al., Nucl. Phys. Proc. Suppl. 77 (1999) 20-25;

[67] K. Muto, H.V. Klapdor, in "Neutrinos", Graduate Texts in Contemporary Physics", ed. H.V. Klapdor, Berlin, Germany: Springer (1988) 183-238.

[68] K. Grotz, H.V. Klapdor, "Die Schwache Wechselwirkung in Kern-, Teilchen- und Astrophysik", B.G. Teubner, Stuttgart (1989), "The Weak Interaction in Nuclear, Particle and Astrophysics", IOP Bristol (1990), Moscow, MIR (1992) and China (1998).

[69] H.V. Klapdor-Kleingrothaus, A. Staudt, "Teilchenphysik ohne Beschleuniger", B.G. Teubner, Stuttgart (1995), "Non–Accelerator Particle Physics", IOP Publishing, Bristol and Philadelphia (1995) and 2. ed. (1998) and Moscow, Nauka, Fizmalit (1998), translated by V.A. Bednyakov.

[70] A. Morales, J. Morales, Nucl. Phys. Proc. Suppl. 114 (2003) 141-157.

[71] F. Simkovic et al., Phys. Rev. C 64 (2001) 035501.

[72] J. Schechter, J.W.F. Valle, Phys. Rev. D 25 (1982) 2951-2954.

[73] M. Hirsch, H.V. Klapdor-Kleingrothaus, Phys. Lett. B 398 (1997) 311; Phys. Rev. D 57 (1998) 1947; M. Hirsch, H.V. Klapdor-Kleingrothaus, St. Kolb, Phys. Rev. D 57 (1998) 2020.

[74] H. Päs, M. Hirsch, H.V. Klapdor-Kleingrothaus, S.G. Kovalenko, Phys. Lett. B 453 (1999) 194-199.

[75] T. Tomoda, Rept. Prog. Phys. 54 (1991) 53-126.

[76] S. Stoica, H.V. Klapdor-Kleingrothaus, Nucl. Phys. A 694 (2001) 269-294.

[77] S. Stoica, H.V. Klapdor-Kleingrothaus, Phys. Rev. C 63 (2001) 064304.

[78] A. Faessler, F. Simkovic, J. Phys. G 24 (1998) 2139-2178.

[79] Yu. Zdesenko et al., Phys. Lett. B 546 (2002) 206-215.

[80] S.R. Elliott, A.A. Hahn, M.K. Moe, Phys. Rev. Lett. 59 (1987) 989.

[81] E. Fiorini et al., Phys. Lett. B 25 (1967) 602.

[82] P. Vogel in PDG (ed. K Hagiwara et al.) Phys. Rev. D 66 (2002) 010001.

[83] C. Weinheimer, in Appec meeting, Karlsrhue, 16-18 September 2003, http://www-ik.fzk.de/%7ekatrin/atw/talks.html, and J. Bonn et al., Nucl. Phys. Proc. Suppl. 110 (2002) 395-397.

[84] A.M. Bakalyarov et al. (Moscow grop of HEIDELBERG-MOSCOW experiment), hep-ex/0309016, hep-ex/0203017.

[85] E. Ma, M. Raidal, Phys. Rev. Lett. 87 (2001) 011802; Erratum-ibid. 87 (2001) 159901 and hep-ph/0102255.

[86] K.S. Babu, E. Ma, J.W.F. Valle, Phys. Lett. B552 (2003) 207-213 and hep-ph/0206292.

[87] E. Ma in Proc. of Intern. Conf. on Physics Beyond the Standard Model: Beyond the Desert 02, BEYOND'02, Oulu, Finland, 2-7 Jun. 2002, IOP, Bristol, 2003, and BEYOND 2003, Ringberg Castle, Tegernsee, Germany, 9-14 Juni 2003, Springer, Heidelberg, Germany, 2003, ed. H.V. Klapdor-Kleingrothaus.

[88] R.N. Mohapatra, M.K. Parida, G. Rajasekaran, (2003) hep-ph/0301234.

[89] D. Fargion et al., in Proc. of DARK2000, Heidelberg, Germany, July 10-15, 2000, Ed. H.V. Klapdor-Kleingrothaus, *Springer*, (2001) 455-468 and in Proc. of Beyond the Desert 2002, BEYOND02, Oulu, Finland, June 2002, IOP 2003, and BEYOND03, Ringberg Castle, Tegernsee, Germany, 9-14 Juni 2003, Springer, Heidelberg, Germany, 2003, ed. H.V. Klapdor-Kleingrothaus.

[90] Z. Fodor, S.D. Katz, A. Ringwald, Phys. Rev. Lett. 88 (2002) 171101 and Z. Fodor et al., *JHEP* (2002) 0206:046, or hep-ph/0203198, and in Proc. of Intern. Conf. on Physics Beyond the Standard Model: Beyond the Desert 02, BEYOND'02, Oulu, Finland, 2-7 Jun 2002, IOP, Bristol, 2003, ed. H V Klapdor-Kleingrothaus and hep-ph/0210123.

[91] KamLAND Coll., Phys. Rev. Lett. 90 (2003) 021802 and hep-ex/0212021.

[92] G.L. Fogli et al., Phys. Rev. D 67 (2003) 073002 and hep-ph/0212127.

[93] J.E. Ruhl et al., astro-ph/0212229.

[94] D.N. Spergel et al., Astrophys. J. Suppl. 148 (2003) 175 and astro-ph/0302209.

[95] A. Pierce and H. Murayama, hep-ph/0302131.

[96] H. V. Klapdor-Kleingrothaus, U. Sarkar, hep-ph/0304032, and in Mod. Phys. Letter. A 18 (2003) 2243-2254.

[97] S. Hannestad, CAP 0305 (2003) 920030 004, and astro-ph/0303076, also see in Proc. of Forth International Conference on Particle Physics Beyond the Standard Model, BEYOND03, Ringberg Castle, Tegernsee, Germany, 9-14 Juni 2003, Springer, Heidelberg, Germany, 2003, ed. H.V. Klapdor-Kleingrothaus.

[98] S.W. Allen, R.W. Schmidt, S.L. Bridle, astro-ph/0306386.

[99] M. Maltoni, T. Schwetz, M.A. Tortola, J.W.F. Valle, hep-ph/0309130.

[100] A. Blanchard, M. Douspis, M. Rowan-Robinson, S. Sarkar, astro-ph/0304237.

[101] H.V. Klapdor-Kleingrothaus in Proceedings of BEYOND'97, First International Conference on Particle Physics Beyond the Standard Model, Castle Ringberg, Germany, 8-14 June 1997, edited by H.V. Klapdor-Kleingrothaus and H. Päs, IOP Bristol (1998) 485 - 531 and in Int. J. Mod. Phys. A 13 (1998) 3953.

[102] H.V. Klapdor-Kleingrothaus, J. Hellmig, M. Hirsch, J. Phys. G 24 (1998) 483-516.

[103] H.V. Klapdor-Kleingrothaus et al. MPI-Report MPI-H-V26-1999, hep-ph/9910205, in Proc. of the 2nd Int. Conf. on Particle Physics Beyond the Standard Model BEYOND'99, Castle Ringberg, Germany, 6-12 June 1999, eds. H.V. Klapdor-Kleingrothaus and I.V. Krivosheina, IOP Bristol (2000) 915-1014.

[104] R. Bernabei et al., Riv. Nuovo Cim. 26 (2003) 1-73.

[105] H.V. Klapdor-Kleingrothaus, M. Hirsch, Z. Phys. A 359 (1997) 361-372.

[106] J. Hellmig, H.V. Klapdor-Kleingrothaus, Z. Phys. A 359 (1997) 351-359 and nucl-ex/9801004.

[107] H V Klapdor-Kleingrothaus 2001 in Proc. Int. Workshop on Low Energy Solar Neutrinos, LowNu2, Dec. 4-5, ed: Y Suzuki et al. World Scientific, Singapore 116-131 and hep-ph/0104028.

[108] I. Bergström, private communication 2003.

[109] G. Gratta, ApPEC (Astroparticle Physics European Coordination), Paris, France 22.01.2002, and in Proc. International Workshop on Low Energy Solar Neutrinos, of LowNu2, Dec. 4-5 (2000) Tokyo, Japan, ed: Y. Suzuki, World Scientific (2001) p.98. home page: http://www-sk.icrr.u-tokyo.ac.jp/neutlowe/2/ transparency/index.html

[110] M. Kirchbach, C. Compean and L. Noriega, hep-ph/0310297, and M. Kirchbach in Proc. of BEYOND03, 4th Int. Conf. on Particle Physics Beyond the Standard Model, Castle Ringberg, Germany, 9-14 June 2003, *Springer* (2004), ed. H V Klapdor-Kleingrothaus.

[111] M. Tegmark et al., astro-ph/0310723.

[112] R. Hofmann, hep-ph/0401017 v.1.